Species diversity in the marine microturbellarian *Astrotorhynchus bifidus* sensu lato (Platyhelminthes: Rhabdocoela) from the Northeast Pacific Ocean

Niels W.L. Van Steenkiste*, Elizabeth R. Herbert, Brian S. Leander

Beaty Biodiversity Research Centre, Department of Zoology, University of British Columbia, 3529-6270 University Blvd, Vancouver, BC V6T 1Z4, Canada

ARTICLE INFO

ABSTRACT

Increasing evidence suggests that many widespread species of meiofauna are in fact regional complexes of (pseudo-)cryptic species. This knowledge has challenged the 'Everything is Everywhere' hypothesis and also partly explains the meiofauna paradox of widespread nominal species with limited dispersal abilities. Here, we investigated species diversity within the marine microturbellarian *Astrotorhynchus bifidus* sensu lato in the Northeast Pacific Ocean. We used a multiple-evidence approach combining multi-gene (18S, 28S, COI) phylogenetic analyses, several single-gene and multi-gene species delimitation methods, haplotype networks and conventional taxonomy to designate Primary Species Hypotheses (PSHs). This included the development of rhabdocoel-specific COI barcode primers, which also have the potential to aid in species identification and delimitation in other rhabdocoels. Secondary Species Hypotheses (SSHs) corresponding to morphospecies and pseudo-cryptic species were then proposed based on the minimum consensus of different PSHs. Our results showed that (a) there are at least five species in the *A. bifidus* complex in the Northeast Pacific Ocean, four of which can be diagnosed based on stylet morphology, (b) the *A. bifidus* complex is a mixture of sympatric and allopatric species with regional and/or subglobal distributions, (c) sympatry occurs on local (sample sites), regional (Northeastern Pacific) and subglobal (Northern Atlantic, Arctic, Northeastern Pacific) scales. Mechanisms for this co-occurrence are still poorly understood, but we hypothesize they could include habitat differentiation (spatial and/or seasonal) and life history characteristics such as sexual selection and dispersal abilities. Our results also suggest the need for improved sampling and exploration of molecular markers to accurately map gene flow and broaden our understanding of species diversity and distribution of microturbellarians in particular and meiofauna in general.

1. Introduction

Marine meiofauna are an important component of earth's biodiversity and play critical roles in ecosystem functioning (Zeppilli et al., 2015). Yet, only a fraction of meiofaunal diversity is known to science (Carugati et al., 2015; Fonseca et al., 2010; Snelgrove, 1999). Current knowledge on their diversity and distribution is heavily biased toward specific sampling localities and efforts, and even well-studied areas can contain relatively high numbers of undescribed species (Curini-Galletti et al., 2012). For many groups, taxonomic expertise is limited and many taxa are hard to identify because of the time-consuming microscopy to recover morphological characters. More recently, DNA taxonomy based mostly on COI and/or ribosomal genes has emerged as a new tool for species identification and species delimitation. As a result, it became clear that many nominal species of meiofauna, including representatives of cyclophorans (Baker et al., 2007), copepods (Garlitska et al., 2012), polychaetes (Westheide and Schmidt, 2003), flatworms

(Scarpa et al., 2016), rotifers (Gómez et al., 2002), gastropods (Jörger et al., 2012), gastrotrichs (Kieneke et al., 2012), nematodes (Derycke et al., 2008) and nemerteans (Leasi et al., 2016), are in fact complexes of cryptic (morphologically indistinguishable) and pseudo-cryptic (*a posteriori* morphologically distinguishable) species. This hidden diversity at the molecular level will significantly increase estimates of biodiversity for many marine taxa and influence our understanding of ecosystem functioning and priorities for conservation (Appeltans et al., 2012).

Although DNA taxonomy is an exciting tool to assess biodiversity, DNA-based species delimitation has methodological challenges (Fontaneto et al., 2015). Most species delimitation studies on meiofauna have used either single-gene or gene cluster datasets and single-gene delimitation methods. Puillandre et al. (2012b) developed a standardized workflow for large-scale species delimitation of hyperdiverse animal groups using the COI barcode as a starting point to formulate primary species hypotheses (PSHs). These PSHs can then be

corroborated with additional information from ribosomal genes, morphology and reciprocal monophyly, leading to SSHs and formal species delimitations. This approach allows for an efficient workflow when sampling coverage is high. Fewer studies have used multi-gene data and multi-gene delimitation methods to generate PSHs. Secondary species hypotheses (SSHs) can then be inferred based on a minimum consensus between independent molecular markers, morphology and phylogeny (Fontaneto et al., 2015). This multiple-evidence approach provides more resolution to smaller datasets with under-sampled taxa and rare specimens (i.e., singletons) (Jörger et al., 2012). It also improves diagnosability and can uncover problems with contamination, pseudogenes, hybridization or introgression. Combining evidence from phylogeny, molecular species delimitation, morphology and other sources (e.g., ecology) allows taxa to be recognized under a unified species concept (De Queiroz, 2007), rather than just one of the primary species concepts (e.g., biological, phylogenetic, morphological) (Adams et al., 2014).

Distribution patterns of meiofauna are poorly understood. Many nominal species of meiofauna seem to either be cosmopolitan or have wide geographical ranges and therefore fit within the Everything is Everywhere' (EiE) hypothesis (Fenchel and Finlay, 2004; Finlay, 2002). However, they represent a unique case known as the 'meiofauna paradox' (Giere, 2009), because, contrary to many prokaryotes and protists, meiofauna often lack active dispersal propagules and dormancy capabilities. The meiofauna paradox and EiE hypothesis are now challenged by DNA taxonomy and phylogeography, providing accumulating evidence of (pseudo-)cryptic species complexes with biogeographical ranges (Fontaneto, 2011; Fontaneto et al., 2015; Leasi and Norenburg, 2014). However, the biogeographical patterns within these complexes are not always clear. Indeed, several studies have shown that (pseudo-)cryptic meiofauna can be composed of allopatric species (Westheide and Schmidt, 2003), sympatric species (Derycke et al., 2008) or, most often, a mix of sympatric and allopatric species (Garlitska et al., 2012; Jörger et al., 2012; Kieneke et al., 2012; Leasi et al., 2016; Meyer-Wachsmuth et al., 2014; Scarpa et al., 2016). In addition, species within the same complex can either be widespread or have more restricted geographical ranges (Tessens, 2012). The lack of a generalized biogeographical concept could be partly explained by the taxonomic and ecological variation of meiofauna. The majority of animal phyla has meiofaunal representatives with their own life history characteristics, such as reproduction, absence/presence of larval stages, absence/presence of dormancy stages, and ecological tolerances associated with different habitats. These can influence their ability to disperse and adapt to new environmental conditions. As such, (pseudo-) cryptic species and biogeographical patterns need to be carefully looked at taxon by taxon.

Here we examine species diversity in the marine microturbellarian *Astrotorhynchus bifidus* sensu lato (s.l.). Microturbellarians occur abundantly in the interstitial habitats of sediments and epiphytically on macro-algae worldwide. Knowledge on their diversity and distribution is still scarce and heavily biased by sampling efforts (Artois et al., 2011). Exact numbers of the global diversity of marine microturbellarians are not available, but should at least surpass 2000 described species. More intensively studied groups of microturbellarians, such as rhabdocoels and proseriates, are known to harbor high levels of undescribed diversity, both among traditional morphospecies (Appeltans et al., 2012; Curini-Galletti et al., 2012) and cryptic species complexes (Casu and Curini-Galletti, 2004; Curini-Galletti and Puccinelli, 1998; Delogu and Curini-Galletti, 2009; Scarpa et al., 2016; Tessens, 2012).

In this study, we provide insight into the *Astrotorhynchus bifidus* species complex from the coasts of British Columbia and Washington. The nominal species is the only representative of *Astrotorhynchus* within Paramesostominae (Rhabdocoela, Dalytyphloplanida). It was previously recorded from the intertidal and subtidal zones in a wide area spanning from the Northwest Atlantic to the White Sea. As such, this is the first record of *A. bifidus* s. l. in the Pacific Ocean. We uncover 5 species in the Northeastern Pacific by combining single-gene and multi-gene species delimitation analyses, haplotype networks, molecular phylogenetic analyses and comparative morphological data. The molecular data include DNA sequences from two ribosomal genes, 18S rRNA and 28S rRNA, and the COI barcode gene. To obtain the latter, new rhabdocoel-specific COI primers were developed. Four species could be formally diagnosed based on stylet morphology, two of which correspond to the previously recognized subspecies *A. bifidus bifidus* and *A. bifidus regulatus*. Insights into patterns of co-occurrence and biogeography are discussed with reference to life history and passive dispersal of meiofaunal flatworms.

2. Material and methods

2.1. Collection and morphological examination of the taxa

Specimens of *A. bifidus* s. l. were collected in 2015–2016 from seaweeds in the rocky intertidal along the Pacific coast of British Columbia (Canada) and Washington (USA), including the Juan de Fuca Strait (Victoria), the Vancouver Island Shelf (Bamfield), the Strait of Georgia (Friday Harbor, Quadra Island), and the North Coast Fjords (Calvert Island) (Fig. 1).

Live animals were isolated from algae using the MgCl$_2$ decantation method (Schockaert, 1996). Specimens were studied alive with the aid of a stereoscope and DIC optics, photographed, and subsequently whole mounted with lactophenol to preserve the stylet of the male genital system. The stylet was then photographed, measured and drawn to examine its morphological details. All pictures were taken with a Zeiss Axioplan 2 microscope equipped with a Zeiss-Axiocam 503-color camera, except for the ones from Calvert Island, which were taken with a Leica DMIL inverted microscope. Pictures of whole mounts in the taxonomic account (Appendix A) were produced in Helicon Focus (HeliconSoft) by stacking series of micrographs. Schematic line art diagrams were drawn freehand based on series of micrographs, scanned and retouched with Inkscape (www.inkscape.org) and GIMP (www. gimp.org). Measurements were taken from whole-mounted and live specimens using ImageJ software (www.imagej.net). From each population (except for Quadra Island), specimens were frozen in a few μL of seawater for DNA extraction.

All type material was deposited in the Beaty Biodiversity Museum (BBM, University of British Columbia, Vancouver, Canada). Metadata on all the specimens of *A. bifidus* s. l., including collection information, DNA, voucher and type material, and access to pictures on morphobank (www.morphobank.org), are given in Table S4.

2.2. DNA extraction, amplification and sequencing

Genomic DNA was extracted from entire specimens with the DNeasy Blood & Tissue kit (Qiagen). Extractions followed manufacturer's instructions except that (a) the AE elution buffer was heated to 60 °C before elution, and (b) DNA was eluted twice for every sample in reduced volumes of 60 μL and 30 μL, respectively.

The COI barcode region (655 bp) of specimens of *A. bifidus* s. l. and all outgroup taxa was amplified with Phusion® Hot Start Flex DNA polymerase (New England Biolabs, Inc.) and the newly developed primers RhCo1F and RhCo1R. In addition, the new COI primers were also tested on 17 other species of rhabdocoels (Table S1). Nearly complete 18S rDNA (1693–1695 bp) and partial 28S rDNA (1568–1656 bp) sequences from all Pacific specimens of *A. bifidus* and the two species of *Promesostoma* were amplified using Illustra™ PuReTaq™ Ready-To-Go™ PCR beads (GE Healthcare) and several different sequencing primer pairs. The 18S and 28S rDNA sequences from the two Atlantic specimens of *A. bifidus* and the other outgroup taxa were mined from Genbank (Table 1). All primers and thermocycling conditions are listed in Table S2. Amplicons were visualized on 1.5% agarose gels stained with
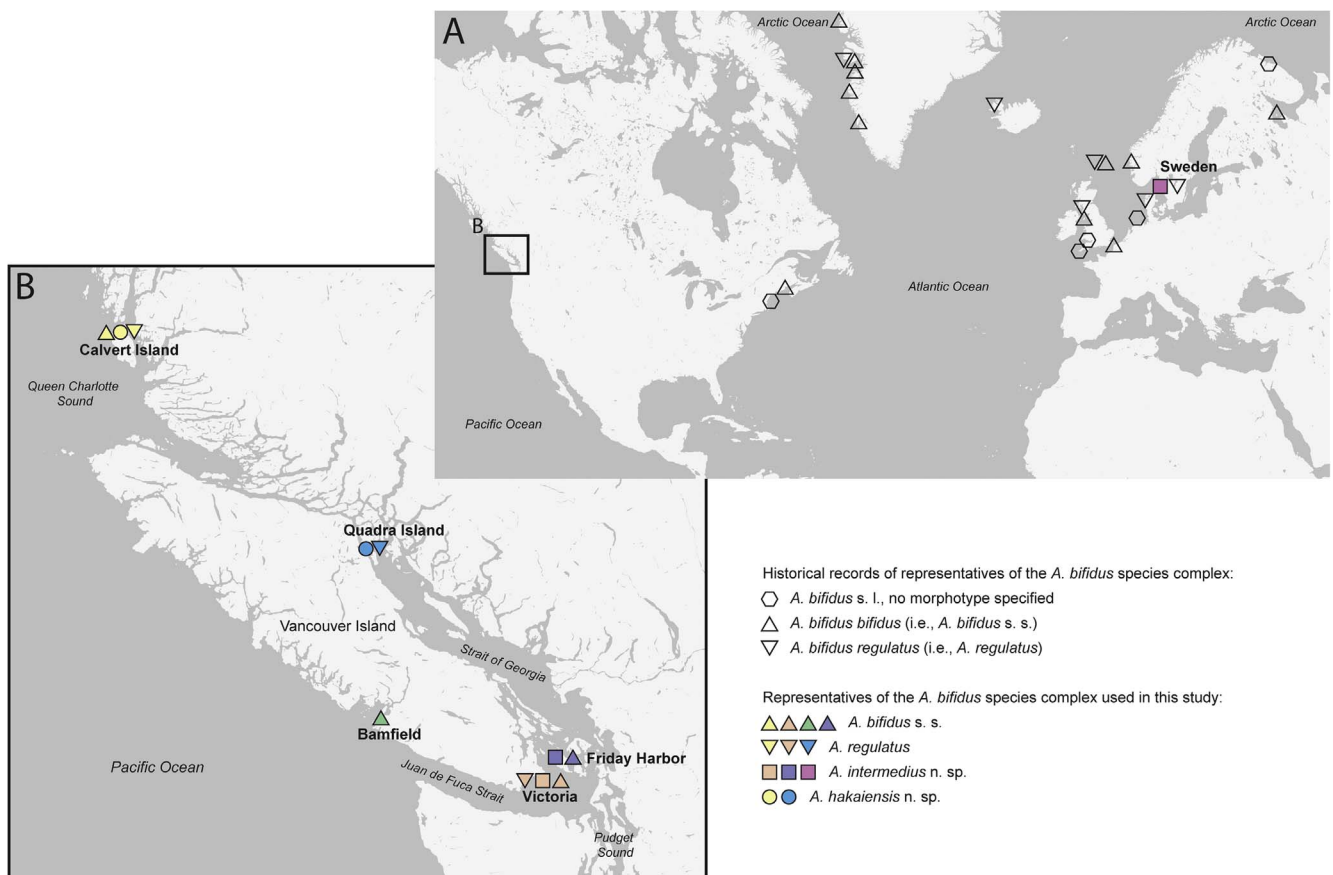
Fig. 1. Global distribution of representatives of the *Astrotorhynchus bifidus* species complex. (A) Global distribution data compiled from the literature. (B) Sampling localities in the Northeast Pacific Ocean. Colors represent different sampling localities and correspond with the colors representing geographic origin in Fig. 4. Symbols represent morphotypes. (For interpretation of the references to color in this figure legend, the reader is referred to the web version of this article.)

GelRed™ (Biotium) and enzymatically cleaned prior to sequencing with Illustra™ ExoProStar S (GE Healthcare).

Clean amplicons were sequenced in 10 μL reactions using the amplification primers (COI, 18S, 28S) and several internal sequencing primers (18S, 28S; Table S2). Sequencing reactions contained 1 μL BigDye® Terminator (BDT) v3.1 (Applied Biosystems), 2 μL BDT buffer, 0.5 μM primer and 1–2 μL PCR product. Sequencing products were cleaned and run on an Applied Biosystems 3730S 48-capillary DNA analyzer by the Nucleic Acid Protein Service Unit (NAPS) at the University of British Columbia. Resulting trace files were assembled into full sequences in Geneious v9.1.5 (www.geneious.com, Kearse et al., 2012) and subjected to a BLAST search on the NCBI website (http://blast.ncbi.nlm.nih.gov) to verify the sample's taxonomic identity. All sequences were deposited in GenBank. Specimen collection data and sequence accession numbers are provided in Table 1.

2.3. Molecular phylogenetic analyses

The COI sequences were aligned in Geneious using the translation option. The 18S and 28S rDNA sequences were aligned using the structural Q-INSI algorithm in MAFFT (Katoh and Toh, 2008). Taxa for the outgroup were chosen based on current knowledge on the phylogenetic relationships within the Thalassotyphloplanida (Van Steenkiste et al., 2013). The COI alignment had no gap regions and required no further trimming or curation. The 5′ and 3′ ends of the 18S and 28S rDNA alignments were trimmed in Geneious. Ambiguous positions were selected with Aliscore v2.2 (Misof and Misof, 2009) and removed from these alignments with Alicut v2.3 (Kueck, 2009). From the resulting three alignments, a concatenated dataset (18S + 28S + COI) was created.

Before running the molecular phylogenetic analyses, best-fit partitioning schemes and models of molecular evolution for the COI alignment and the concatenated alignment were recovered in PartitionFinder v.1.1.0 using a greedy search with PhyML and the Akaike (AIC) and Bayesian (BIC) information criteria (Lanfear et al., 2012). In case of incongruence between the AIC and BIC best model, the most complex model was chosen. These partition schemes and models of evolution were used in all subsequent phylogenetic analyses and are listed in Table S3. Maximum likelihood and two Bayesian analyses were done in RAxML v8.2.9 (Stamatakis, 2014), MrBayes v3.2.6 (Ronquist and Huelsenbeck, 2003) and the BEAST 2 package (Bouckaert et al., 2014), respectively, on XSEDE in the CIPRES Science Gateway v3.3 (https://phylo.org). RAxML best-scoring ML tree search and non-parametric bootstrapping (1000 replicates) were performed on the partitioned concatenated alignment. MrBayes partitioned Bayesian analyses were done on the 18S, 28S and partitioned COI datasets separately and on the partitioned concatenated dataset, using default prior and mcmc settings, in two independent simultaneous runs for 100 million generations. Trees were sampled every 1000th generation after a 25% burnin. LogL values and the average deviation of split frequencies were considered as convergence diagnostics. The remaining 75,000 trees were summarized in a 50% majority rule consensus tree. Three standard BEAST 2 input files were generated in BEAUti 2 for the 18S, 28S and partitioned COI datasets, respectively. For all datasets, we selected the uncorrelated lognormal relaxed clock model and a constant population coalescent tree prior. Three independent mcmc chains were run for 2 billion generations with a sample frequency of 4000. Mixing, convergence and burnin of the mcmc chains was evaluated by examining the effective sample size (ESS) and traces of the different parameters in Tracer v1.6.1 (Rambaut et al., n.d.). Tree files of the best run for each dataset were thinned by a factor 50 after a 50% burnin in

Table 1
18S rRNA, 28S rRNA and COI GenBank accession numbers, localities and geographic coordinates of the taxa used in the analyses.

Taxa	Locality	Coordinates	Collection date	18S accession #	28S accession #	COI accession #	Reference
Ingroup							
Astrotorhynchus bifidus (McIntosh, 1875) von Graff, 1905							
CI33	Calvert Island, BC	51°39′52″N; 128°05′47″W	June 6, 2015	MG256028	MG256072	MG256124	Present study
CI38	Calvert Island, BC	51°39′52″N; 128°05′47″W	June 6, 2015	MG256029	MG256073	MG256125	Present study
CI39	Calvert Island, BC	51°39′52″N; 128°05′47″W	June 6, 2015	MG256030	MG256074	MG256126	Present study
CI68	Calvert Island, BC	51°39′52″N; 128°05′47″W	June 6, 2015	MG256031	MG256075	MG256127	Present study
CI69	Calvert Island, BC	51°39′52″N; 128°05′47″W	June 6, 2015	MG256032	MG256076	MG256128	Present study
CI174	Calvert Island, BC	51°39′52″N; 128°05′47″W	April 10, 2016	MG256033	MG256077	MG256129	Present study
CI175	Calvert Island, BC	51°39′07″N; 128°08′33″W	April 9, 2016	MG256034	MG256078	MG256130	Present study
Vic4	Victoria, BC	48°24′12″N; 123°21′03″W	March 20, 2015	MG256041	MG256085	MG256144	Present study
Vic23	Victoria, BC	48°24′12″N; 123°21′03″W	March 20, 2015	MG256042	MG256086	–	Present study
Vic65	Victoria, BC	48°24′12″N; 123°21′03″W	March 20, 2015	MG256043	MG256087	MG256145	Present study
Vic66	Victoria, BC	48°24′12″N; 123°21′03″W	March 20, 2015	MG256044	MG256088	MG256146	Present study
Vic67	Victoria, BC	48°24′12″N; 123°21′03″W	March 20, 2015	MG256045	MG256089	MG256147	Present study
Vic73	Victoria, BC	48°24′12″N; 123°21′03″W	September 2, 2015	MG256046	MG256090	MG256148	Present study
Vic74	Victoria, BC	48°24′12″N; 123°21′03″W	September 2, 2015	MG256047	MG256091	MG256149	Present study
Vic75	Victoria, BC	48°24′12″N; 123°21′03″W	September 2, 2015	MG256048	MG256092	MG256150	Present study
Vic154	Victoria, BC	48°24′12″N; 123°21′03″W	March 3, 2016	MG256049	MG256093	MG256151	Present study
Vic155	Victoria, BC	48°24′12″N; 123°21′03″W	March 3, 2016	MG256050	MG256094	MG256152	Present study
Vic156	Victoria, BC	48°24′12″N; 123°21′03″W	March 3, 2016	MG256051	MG256095	MG256153	Present study
Vic238	Victoria, BC	48°24′12″N; 123°21′03″W	November 2, 2016	MG256052	MG256096	MG256154	Present study
Vic239	Victoria, BC	48°24′12″N; 123°21′03″W	November 2, 2016	MG256053	MG256097	MG256155	Present study
Vic240	Victoria, BC	48°24′12″N; 123°21′03″W	November 2, 2016	MG256054	MG256098	MG256156	Present study
Vic241	Victoria, BC	48°24′12″N; 123°21′03″W	November 2, 2016	MG256055	MG256099	MG256157	Present study
Vic242	Victoria, BC	48°24′12″N; 123°21′03″W	November 2, 2016	MG256056	MG256100	MG256158	Present study
Vic244	Victoria, BC	48°24′12″N; 123°21′03″W	February 5, 2017	MG256057	MG256101	MG256159	Present study
Vic245	Victoria, BC	48°24′12″N; 123°21′03″W	February 5, 2017	MG256058	MG256102	MG256160	Present study
Vic246	Victoria, BC	48°24′12″N; 123°21′03″W	February 5, 2017	MG256059	MG256103	MG256161	Present study
Vic247	Victoria, BC	48°24′12″N; 123°21′03″W	February 5, 2017	MG256060	MG256104	MG256162	Present study
Vic248	Victoria, BC	48°24′12″N; 123°21′03″W	February 5, 2017	MG256061	MG256105	MG256163	Present study
Vic249	Victoria, BC	48°24′12″N; 123°21′03″W	February 5, 2017	MG256062	MG256106	MG256164	Present study
Vic250	Victoria, BC	48°24′12″N; 123°21′03″W	February 5, 2017	MG256063	MG256107	MG256165	Present study
Vic251	Victoria, BC	48°24′12″N; 123°21′03″W	February 5, 2017	MG256064	MG256108	MG256166	Present study
Vic252	Victoria, BC	48°24′12″N; 123°21′03″W	February 5, 2017	MG256065	MG256109	–	Present study
Vic253	Victoria, BC	48°24′12″N; 123°21′03″W	February 5, 2017	MG256066	MG256110	MG256167	Present study
BF46	Bamfield, BC	48°51′05″N; 125°07′19″W	July 2, 2015	MG256024	MG256067	MG256115	Present study
BF61	Bamfield, BC	48°51′05″N; 125°07′19″W	July 2, 2015	MG256025	MG256068	MG256116	Present study
BF62	Bamfield, BC	48°51′05″N; 125°07′19″W	July 2, 2015	MG256026	MG256069	MG256117	Present study
BF63	Bamfield, BC	48°51′05″N; 125°07′19″W	July 2, 2015	MG256027	MG256070	MG256118	Present study
BF64	Bamfield, BC	48°51′05″N; 125°07′19″W	July 2, 2015	–	MG256071	MG256119	Present study
FH233	Friday Harbor, WA	48°32′42″N; 123°00′44″W	October 8, 2016	MG256035	MG256079	MG256132	Present study
FH234	Friday Harbor, WA	48°32′42″N; 123°00′44″W	October 8, 2016	MG256036	MG256080	MG256133	Present study
FH235	Friday Harbor, WA	48°32′42″N; 123°00′44″W	October 8, 2016	MG256037	MG256081	MG256134	Present study
FH236	Friday Harbor, WA	48°32′42″N; 123°00′44″W	October 8, 2016	MG256038	MG256082	MG256135	Present study
KC529551	Gåsevik, Sweden	58°14′46″N; 11°26′13″E	–	KC529551	KC529551	–	Van Steenkiste et al., 2013
AJ312270	Bohuslän, Sweden	–	–	AJ312270	–	–	Noren and Jondelius, 2002
Outgroup							
Promesostoma sp.	Calvert Island, BC	51°39′50″N; 128°08′43″W	June 7, 2015	MG256040	MG256084	MG256141	Present study
Promesostoma dipterostylum Karling, 1967	Nanaimo, BC	49°11′43″N; 123°57′32″W	April 12, 2015	MG256039	MG256083	MG256140	Present study
Ceratopera complicata Van Steenkiste and Leander, 2017	Victoria, BC	48°24′12″N; 123°21′03″W	November 14, 2016	MF321747	MF321757	MG266158	Van Steenkiste and Leander, 2017; present study
Ceratopera pacifica (Karling, 1986) Van Steenkiste and Leander, 2017	Bamfield, BC	48°51′05″N; 125°07′19″W	July 2, 2015	MF321748	MF321758	MG266159	Van Steenkiste and Leander, 2017; present study

Table 1 (continued)

Taxa	Locality	Coordinates	Collection date	18S accession #	28S accession #	COI accession #	Reference
Ceratopera pilifera Karling, 1986	Victoria, BC	48°24′12″N; 123°21′03″W	November 14, 2016	MF321749	MF321759	MG266160	Van Steenkiste and Leander, 2017; present study
Trigonostomum tori (Karling, 1986) Willems et al., 2004	Victoria, BC	48°24′12″N; 123°21′03″W	May 6, 2015	MF321754	MF321763	MG266163	Van Steenkiste and Leander, 2017; present study
Ptychopera unicornis Van Steenkiste and Leander, 2017	Victoria, BC	48°24′12″N; 123°21′03″W	September 2, 2015	MF321752	MF321761	MG266162	Van Steenkiste and Leander, 2017; present study
Ptychopera japonica Ax, 2008	Surrey, BC	49°05′09″N; 122°51′39″W	July 29, 2015	MF321751	MF321760	MG266161	Van Steenkiste and Leander, 2017; present study
Tvaerminnea karlingi Luther, 1943	Nanaimo, BC	49°11′43″N; 123°57′32″W	April 12, 2015	MF321755	MF321764	MG266164	Van Steenkiste and Leander, 2017; present study

LogCombiner v2.4.4. A maximum clade credibility tree was built from these 10,000 trees in TreeAnnotator v2.4.4 with default settings. Threshold values for support are 70% for bootstrap (Hillis and Bull, 1993) and 0.95 for posterior probabilities (Huelsenbeck and Rannala, 2004).

2.4. Species delimitation

2.4.1. Single-gene methods

We applied three different molecular-based methods for species delimitation: (a) the Poisson Tree Process (PTP) method of Zhang et al. (2013); (b) the General Mixed Yule Coalescent (GMYC) method of Pons et al. (2006); and (c) the Automatic Barcode Gap Discovery (ABGD) method of Puillandre et al. (2012a). These methods were implemented on each of the single-locus datasets. Identical sequences were removed in all datasets prior to the analyses.

The PTP method delimits species based on the phylogenetic species concept and requires phylograms as input trees. We implemented the Bayesian bPTP on a subset of 1000 trees sampled from the MrBayes analyses. Using multiple trees can account for uncertainties in phylogenetic inference. Settings for the bPTP analyses were 100,000 mcmc iterations with a sampling frequency of 100 and a burnin of 25%. The bPTP was run in Python using the ETE package (available from https://github.com/zhangjiajie/PTP).

The GMYC method detects the transition from an intra-specific coalescent process to a speciation process and requires ultrametric trees. To account for phylogenetic uncertainty, we ran the Bayesian bGMYC method (Reid and Carstens, 2012) in R on a subset of 1000 ultrametric trees obtained from the BEAST 2 trees after a 50% burnin. Species probabilities results were plotted on the maximum credibility trees obtained earlier.

The ABGD method delimits species based on a barcode gap in the distribution of pairwise genetic differences. The single-locus and concatenated alignments were uploaded on the ABGD web server (http://wwwabi.snv.jussieu.fr/public/abgd/abgdweb.html) and run using default settings.

2.4.2. Multi-gene methods

We verified the PSHs proposed by the single-gene species delimitation methods with two different multi-locus species delimitation approaches: (a) the Bayesian Phylogenetics and Phylogeography (BPP) method of Yang (2015); and (b) the Species Tree And Classification Estimation, Yarely (STACEY) method of Jones (2017). Both multi-locus methods operate within a Bayesian framework and use a phylogenetic species tree as a guide tree.

The BPP method compares several models of species delimitation and phylogeny in a Bayesian framework under a multispecies coalescent model. Three additional species trees were obtained in the BEAST 2 package using the multispecies coalescent *BEAST method (Heled and Drummond, 2010). The input files were generated in BEAUti 2 using the *BEAST with STACEY option template. The concatenated dataset was used as input alignment with partitions and site models previously obtained in PartitionFinder. *A. bifidus* s. l. sequences were assigned to 5, 7 and 8 putative species as delineated in the single-gene species delimitation analyses on the 28S and COI datasets. DNA sequences from the outgroup were each assigned to their own species resulting in taxon sets of 14, 16 and 17 species for each BEAUti 2 input file, respectively. We selected the uncorrelated lognormal relaxed clock model for each partition and the Yule model species tree prior. Improper 1/X priors were changed to lognormal ones. The mcmc settings, evaluation of the parameters and tree building were identical to the BEAST 2 analyses described earlier. After the completion of the analyses on CIPRES, three sets of BPP analyses were run, each using a different *BEAST species tree as a guide tree. To account for the influence of priors θ (ancestral population size) and τ (divergence time), 4 different prior combinations were tested for each set: (a) gamma priors G(1, 10) for both θ and τ,

suggesting a large ancestral populations size and deep relative divergences; (b) G(1, 10) for θ and G(2, 2000) for τ, suggesting a large ancestral population size and shallow relative divergences; (c) G(2, 2000) for θ and G(1, 10) for τ, suggesting a small ancestral population size and deep relative divergences; and (d) G(2,2000) for both θ and τ, suggesting a small ancestral population size and shallow relative divergences. The remaining divergence time parameters were assigned the Dirichlet prior. Analyses were run for 100,000 generations sampling every 5 generations with a burnin of 10,000. All analyses were run in triplicate to verify consistency.

The STACEY method uses a threshold and birth-death-collapse model to delineate species in a Bayesian framework under a multi-species coalescent model. Similar to the *BEAST analyses above, 3 input files were generated in the BEAUti 2 STACEY template using the same partitions, putative species assignments, prior and mcmc settings, and site, clock and tree models. The Collapse Height prior and Relative Death Rate were set to 0.00001 and 0, respectively. Cluster analyses of the resulting Species or Minimal Clusters (SMC) trees (250,000 trees after a 50% burnin) were done using Species-Delimitation-Analyzer (Jones et al., 2015) with collapse-height set to the same value as in STACEY and simcutoff set to 1.

2.5. Genetic distances and statistical parsimony networks

Uncorrected p-distances between *A. bifidus* s. l. haplotype pairs within and between haplogroups (corresponding with the 5 PSHs retrieved from the species delimitation analyses), were calculated in MEGA v7 (Kumar et al., 2016). New alignments were made for every gene in MAFFT as described above, excluding identical sequences and the outgroup taxa.

Haplotype connectivity was explored through haplotype networks using statistical parsimony. Only 28S rDNA and COI datasets, including identical sequences, were used. 18S rDNA sequences displayed lower haplotype diversity and proved less suitable for species delimitation of closely related taxa. A 95% parsimony criterion was applied in TCS v1.21 (Clement et al., 2000) to both datasets to delimit PSHs. Statistical parsimony TCS networks were visualized in PopART (available from http://popart.otago.ac.nz).

3. Results

3.1. DNA taxonomy

The new COI primers, RhCo1F and RhCo1R, successfully amplified a 652–661 bp-long COI fragment in the *A. bifidus* s. l. specimens, the outgroup taxa (all dalytyphloplanids) and 17 other species of rhabdocoels (2 dalytyphloplanids and 15 kalyptorhynchs; Table S1). This fragment corresponded with the standard COI barcode (i.e., the Folmer fragment) of other metazoans. Sequence lengths of the newly sequenced *A. bifidus* s. l. ribosomal amplicons varied between 1683–1695 bp for 18S rDNA using primer pair Prom18SFb/Prom18SRb and between 1568–1572 bp and 1653–1656 bp for 28S using primer pairs BifidusF1/BifidusR1 and LSU5/LSUD6-3B, respectively. The final 18S rDNA, 28S rDNA and COI datasets, including the outgroup taxa, contained 51, 52, and 49 sequences and were 1705 bp, 1631 bp and 655 bp, respectively. This resulted in a concatenated 18S + 28S + COI dataset of 53 sequences with a total length of 3991 bp. The 18S rDNA, 28S rDNA and COI data contain 6, 16 and 29 haplotypes for *A. bifidus* s. l., respectively. Minimum, maximum and mean uncorrected p-distances between haplotypes within and between the haplogroups (resulting from the species delimitation analyses and haplotype networks below) are presented in Table 2. These data clearly show a 'barcode' gap when comparing distances within and between haplogroups for all genes.

3.2. Primary Species Hypotheses (PSH)

3.2.1. Molecular phylogeny

Results of the phylogenetic analyses of the 18S + 28S + COI dataset are shown in Fig. 2A. Bayesian and ML topologies were nearly identical and showed that *A. bifidus* s. l. consists of several monophyletic groups with high support values. Four of these clades corresponded with a distinct morphotype of *A. bifidus* s. l., all of which display bootstrap support (bs) of 100% and posterior probabilities (pp) of 1.0. The phylogenetic relationships among the clades of *A. bifidus* s. l. showed that only maximum likelihood supports clade 1 as the sister group of all other clades (bs = 87, pp = 0.93). Clades 3, 4 and 5 all had high support (bs = 100, pp = 1). One specimen from Victoria (Vic66) did not branch within any of these clades and formed the sister lineage of clade 3. Clades 4 and 5 were well-supported sister lineages (bs = 100, pp = 1). The phylogenetic relationships among the outgroup taxa and between the outgroup and the ingroup were congruent with the results of Van Steenkiste et al. (2013).

3.2.2. Single-gene species delimitation

The single-gene methods suggested different numbers of PSHs depending on the locus and method used (Fig. 2B–D). For the 18S rDNA sequences, the bPTP and bGMYC methods indicated that all *A. bifidus* sequences belong to a single PSH, while the ABGD method recovered 3 PSHs (Fig. 2B). However, all single-gene methods failed to identify the outgroup taxa as separate species for this gene. Consequently, the PSHs recovered by the 18S rRNA were not considered for multigene speciation models. For the 28S rDNA sequences, all methods identified 5 PSHs, 4 clusters (PSH-1, PSH-3, PSH-4, PSH-5) and 1 singleton (PSH-2) (Fig. 2C). The ABGD method did not discriminate *C. complicata* and *C. pacifica* from the outgroup as separate species. For the COI gene, bPTP and bGMYC identified 8 PSHs, 4 clusters (PSH-1a, PSH-3, PSH-4b, PSH-5) and 4 singletons (PSH-1b, PSH-2, PSH-4a, PSH-4b), while the ABGD method recovered 7 PSHs, 4 clusters (PSH-1, PSH-3, PSH-4b, PSH-5) and 3 singletons (PSH-2, PSH-4a, PSH-4b) (Fig. 2D). All COI PSHs were nested within the 28S rDNA PSHs.

3.2.3. Multi-gene species delimitation

The multi-gene methods BPP and STACEY were applied to the PSHs of the 28S rRNA (5 PSHs) and COI (7 and 8 PSHs) single-gene methods. Both methods favored the model with 5 PSHs (Fig. 3A) over the models with 7 and 8 PSHs (Fig. 3B and C). The BPP prior values for θ (ancestral population size) and τ (divergence time) had a significant effect on the outcome of the BPP analyses, giving higher support values when small ancestral population sizes and shallow relative divergences were assumed (Fig. 3). Support for a speciation event was considered strong when pp ≥ 0.95. Nodes representing speciation events leading to PSH-1, PSH-2, PSH-3, PSH-4 and PSH-5 consistently had posterior probabilities of 1 in all three models. Nodes representing speciation events between PSH-1a and PSH-1b, and between PSH-4a, PSH-4b and PSH-4c, respectively (Fig. 3B and C), had either no (pp < 0.90) or weak (0.90 ≤ pp < 0.95) support, except for the speciation event between PSH-4c and PSH-4a/PSH-4b in the model with 7 PSHs and G(2, 2000) for θ and τ (pp = 0.994; Fig. 3B). Results from the STACEY analyses also showed a higher pp-value for the true clustering (i.e., the number of clusters equals the proposed number of PSHs) in the model with 5 PSHs (pp = 0.997) than for the true clustering in the models with 7 PSHs (pp = 0.839) and 8 PSHs (pp = 0.700) (Fig. 3).

3.2.4. Statistical parsimony networks

The delimitation results using the 95% parsimony criterion in TCS recovered 5 PSHs and 8 PSHs in the 28S rDNA and COI datasets, respectively (data not shown). This is consistent with the findings of the other single-gene methods. PSH-1–PSH-5 recovered in our species delimitation analyses formed distinct haplogroups in the PopART TCS haplotype networks (Fig. 4). However, the 28S rDNA (Fig. 4A) and COI

Table 2
Uncorrected p-distances [min–max (mean)] between haplotype pairs within (bold) and between *Astrotorhynchus bifidus* s. l. haplogroups calculated in MEGA v7.

18S	*A. hakaiensis* n. sp.	*A.* sp. 2	*A. regulatus*	*A. bifidus* s. s.	*A. intermedius* n. sp.
A. hakaiensis n. sp.	**0.000–0.000 (0.000)**				
A. sp. 2	0.013–0.013 (0.013)	NA			
A. regulatus	0.015–0.015 (0.015)	0.004–0.004 (0.004)	**0.000–0.000 (0.000)**		
A. bifidus s. s.	0.015–0.015 (0.015)	0.020–0.020 (0.020)	0.022–0.022 (0.022)	**0.000–0.000 (0.000)**	
A. intermedius n. sp.	0.012–0.012 (0.012)	0.017–0.017 (0.017)	0.020–0.020 (0.020)	0.005–0.005 (0.005)	**0.000–0.000 (0.000)**
28S	*A. hakaiensis* n. sp.	*A.* sp. 2	*A. regulatus*	*A. bifidus* s. s.	*A. intermedius* n. sp.
A. hakaiensis n. sp.	**0.000–0.001 (0.000)**				
A. sp. 2	0.038–0.040 (0.039)	NA			
A. regulatus	0.038–0.042 (0.040)	0.011–0.012 (0.012)	**0.000–0.001 (0.000)**		
A. bifidus s. s.	0.047–0.048 (0.047)	0.044–0.044 (0.044)	0.045–0.047 (0.046)	**0.000–0.000 (0.000)**	
A. intermedius n. sp.	0.047–0.049 (0.048)	0.043–0.043 (0.043)	0.047–0.050 (0.048)	0.024–0.026 (0.026)	**0.000–0.003 (0.001)**
COI	*A. hakaiensis* n. sp.	*A.* sp. 2	*A. regulatus*	*A. bifidus* s. s.	*A. intermedius* n. sp.
A. hakaiensis n. sp.	**0.003–0.053 (0.028)**				
A. sp. 2	0.197–0.203 (0.200)	NA			
A. regulatus	0.185–0.202 (0.195)	0.171–0.176 (0.173)	**0.000–0.014 (0.006)**		
A. bifidus s. s.	0.203–0.239 (0.210)	0.192–0.217 (0.197)	0.177–0.211 (0.186)	**0.000–0.118 (0.025)**	
A. intermedius n. sp.	0.163–0.173 (0.170)	0.169–0.171 (0.171)	0.157–0.168 (0.164)	0.180–0.195 (0.188)	**0.000–0.003 (0.002)**

(Fig. 4B) networks showed different connectivity patterns between these 5 PSHs. Our genetic data showed very limited spatial structure. The geographic origin of the two largest haplogroups, PSH-3 and PSH-4, is mixed, with PSH-4 present in all Pacific locations. PSH-5 was only found in Victoria, but the 28S rDNA data also include a Genbank-mined specimen from Sweden suggesting a much wider geographic distribution. PSH-1 was only found on Calvert Island and Quadra Island (no molecular data is available for the Quadra Island specimens).

3.2.5. Morphology

Astrotorhynchus bifidus s. l. is easily distinguished from other rhabdocoels by its pointed, muscular, proboscoid anterior end, its bifurcated tail, and a male copulatory organ provided with a long stylet with a conspicuous spiral edge. Four morphotypes were distinguished based on differences in stylet morphology. Short descriptions of each morphotype were placed in the taxonomic account within the Appendix A. These morphotypes corresponded with PSH-1, PSH-3, PSH-4 and PSH-5, respectively (Fig. 2F). No morphotype could be retrieved for PSH-2, because of a lack of voucher material for this singleton. In addition to variations in stylet morphology, the general appearance of the PSH-1 morphotype was also distinctly different from all other morphotypes. PSH-3, PSH-4 and PSH-5 morphotypes ranged from transparent to opaque orange-brown, while the PSH-1 morphotype was white-yellow with (usually 2) bright-purple, subepidermal pigment bands (Fig. 2F). The bands were arranged either longitudinally or transversely across the dorsal side of the animal.

3.3. Secondary Species Hypotheses (SSH)

SSHs were determined based on the consensus of the PSHs resulting from reciprocal monophyly, single-gene and multi-gene species delimitation methods, morphology, and haplotype networks. As such, 5 SSHs corresponding to PSH-1, PSH-2, PSH-3, PSH-4, and PSH-5 were recognized. Based on morphotype, two of those, SSH-3 and SSH-4, corresponded to existing names in the literature, i.e., *A. bifidus bifidus* and *A. bifidus regulatus*, respectively (von Graff, 1905). These taxa were previously considered subspecies of *A. bifidus* based on differences in stylet morphology, but are now considered separate species within the *A. bifidus* species complex. The type species of *Astrotorhynchus*, i.e., *Mesostomum bifidum* McIntosh, 1875, belongs to *A. bifidus bifidus* (see von Graff, 1913). The latter will here be referred to as *A. bifidus* s. s. *A. bifidus regulatus* is given full species status as *A. regulatus*. SSH-1 and SSH-5 are recognized as new species, *A. hakaiensis* n. sp. and *A.*

intermedius n. sp., and can also be diagnosed based on stylet morphology. SSH-2 was also supported as a new species, but its nominal species status remains somewhat problematic as it is based on a singleton and no morphological data are available. Therefore it is provisionally named *Astrotorhynchus* sp. 2.

4. Discussion

4.1. DNA taxonomy

The lack of primers for markers other than ribosomal genes has prevented the use of other molecular markers for rhabdocoels. The 'universal' Folmer primers LCO1490 and HCO2198 that amplify the COI barcode in metazoans have been problematic for flatworms because of mismatches in the primer binding sites (Van Steenkiste et al., 2015; Vanhove et al., 2013). The new COI barcode primers presented here were successful in amplifying the first ± 655 bp of the COI gene in a wide taxonomic diversity of rhabdocoels, both dalytyphloplanids and kalyptorhynchs. As such, these primers can provide a useful tool to build COI reference libraries for potential specimen identification of rhabdocoels in the future. Larger COI datasets will allow us to evaluate intraspecific and interspecific variation and test its usefulness as a barcode marker (i.e., whether or not a barcode gap exists). In addition, our results show that the COI barcode can be useful for species delimitation and provide additional resolution to molecular phylogenies of rhabdocoels. The latter have been exclusively based on ribosomal markers with relatively low intrageneric resolution (Tessens et al., 2014; Van Steenkiste et al., 2013). As such, COI could help in elucidating interspecific relationships in some of the most species-rich genera and nominal species that are likely (pseudo-)cryptic species complexes.

4.2. Species delimitation and diversity

Our single-gene species delimitation results show different speciation scenarios for each gene. Not only do the 18S rDNA sequences clearly fail to discriminate between the species of *A. bifidus* s. l., but they also fail to separate clearly diagnosable species from the outgroup. This underestimation of the 'true' number of species by the 18S rRNA gene has also been shown for other taxa of meiofauna (Tang et al., 2012). The 5 PSHs from the partial 28S rRNA analyses are corroborated by the results from all other analyses (multi-gene, reciprocal monophyly, morphology). Although this gene seems very promising for
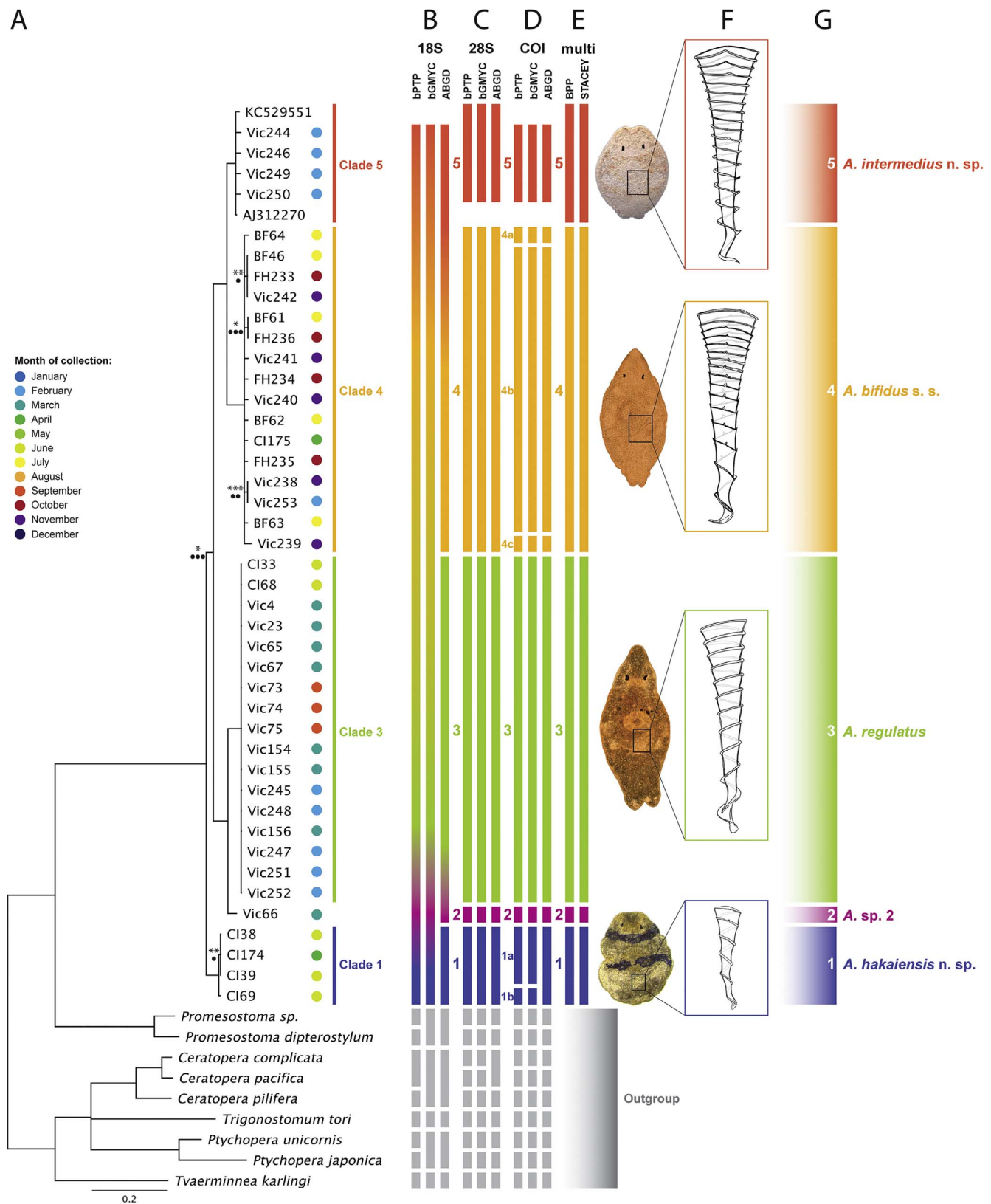
Fig. 2. Species delimitation within the *Astrotorhynchus bifidus* species complex. (A) Bayesian majority-rule consensus tree of the concatenated 18S + 28S + COI alignment. Symbols above branches indicate posterior probabilities (pp) from the Bayesian analysis ($0.90 \leq$ * < 0.95, $0.95 \leq$ ** < 0.97, $0.97 \leq$ *** < 1). Symbols below branches represent bootstrap values (bs) from the maximum likelihood analysis ($60 \leq$ • < 75, $75 \leq$ •• < 85, $85 \leq$ ••• < 100). Branches without symbols are fully supported (pp = 1, bs = 100) while branches below the lowest support threshold (pp < 0.90, bs < 60) have been collapsed. Scale bar represents substitutions per site. Colored circles behind each individual represent the month of collection. (B–D) Single-gene species delimitation analyses: (B) 18S rRNA, (C) 28S rRNA, (D) COI. (E) Multi-gene species delimitation analyses. (F) Stylet morphology of different morphotypes. (G) SSH from PSHs consensus with formal nominal species designation.
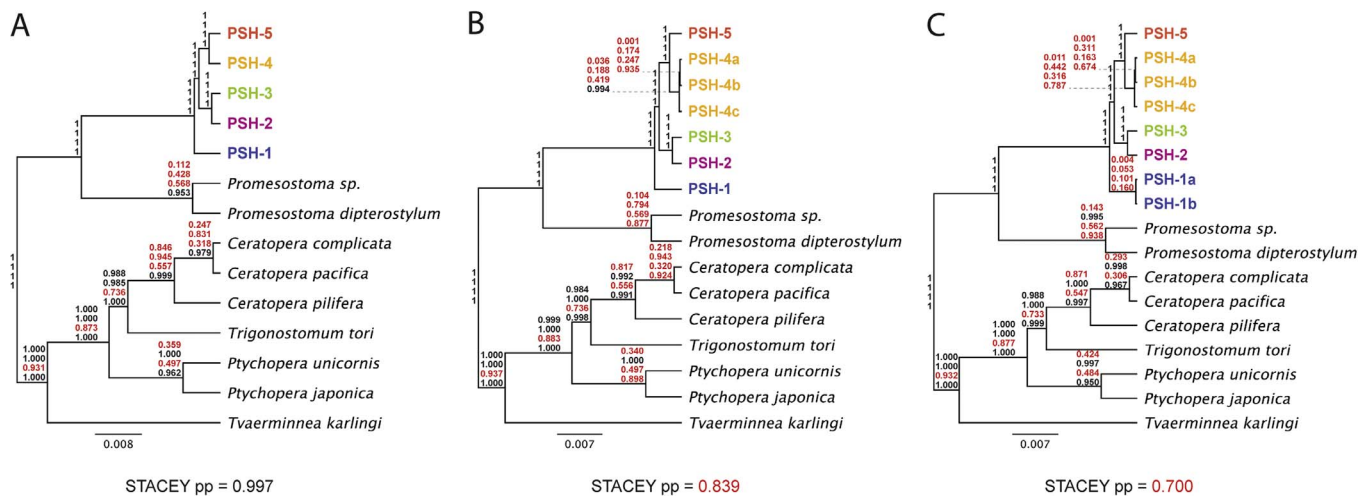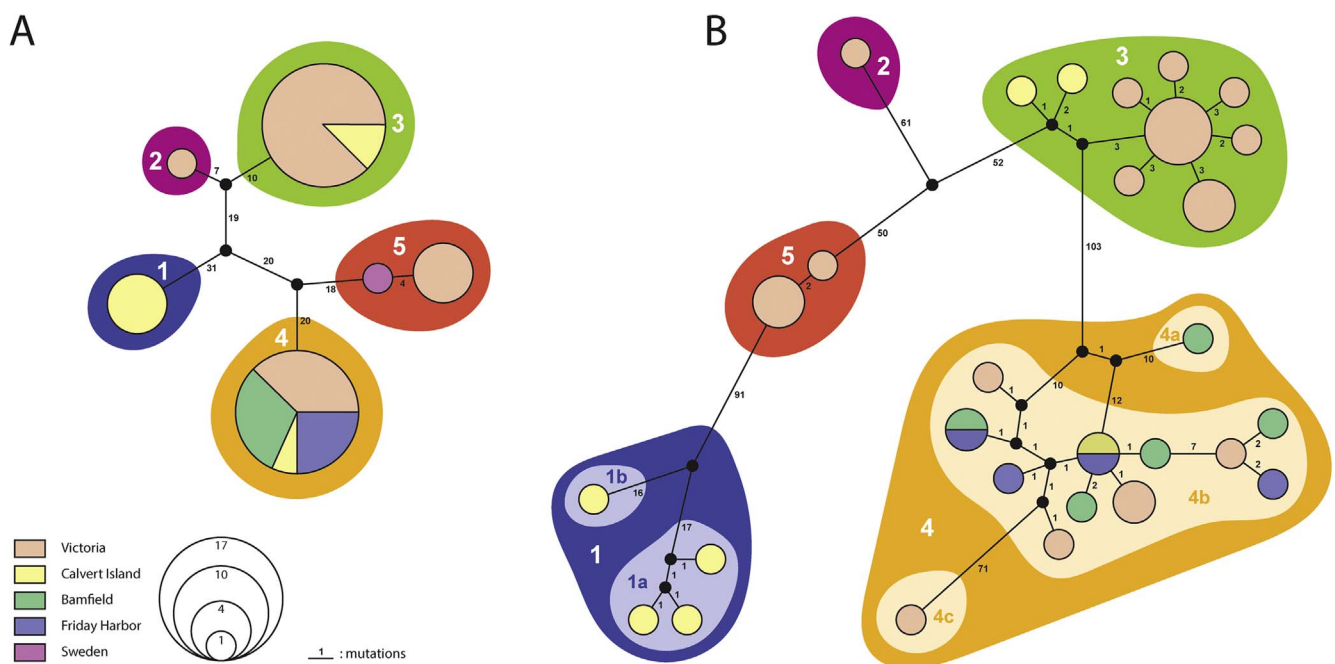
Fig. 3. Multi-gene species delimitation. BPP and STACEY were applied to: (A) the 5 PSHs resulting from the 28S rRNA single-gene methods, (B) the 7 PSHs from the COI ABGD method, and (C) the 8 PSHs from the COI bPTP and bGMYC methods. Posterior probability (pp) support values for speciation events from the BPP analyses are plotted on the nodes of *BEAST maximum clade credibility trees under different prior combinations of θ (ancestral population size) and τ (divergence time). Upper to lower pp-values: G(1, 10) for both θ and τ; G(1, 10) for θ and G(2, 2000) for τ; G(2, 2000) for θ and G(1, 10) for τ; G(2, 2000) for both θ and τ. STACEY pp-values for the models with 5, 7 and 8 PSHs, respectively, are shown below each tree. pp-values < 0.95 are in red. Colors of PSHs refer to the different species of *Astrotorhynchus* in Fig. 2. (For interpretation of the references to color in this figure legend, the reader is referred to the web version of this article.)

species delimitation and DNA barcoding in rhabdocoels, the sequence length (1600 bp) could pose challenges for high-throughput sequencing and contig assembly. For the COI gene, several PSHs were not supported by reciprocal monophyly and multi-gene delimitation. However, because of the low 'intraspecific' resolution of our multi-gene phylogenetic analyses and the lack of verified morphotypes for every specimen within each SSH, it would be preliminary to conclude COI overestimates the number of 'true' species. More taxa and markers are needed to verify whether these COI-based PSHs merely capture intraspecific variation or represent 'true' species. Such additional independent molecular markers (mitochondrial and/or nuclear genes) could also be useful to test for gene flow, hybridization and

introgression and, as such, strengthen the recognition of valid species under a unified species concept (De Queiroz, 2007).

With only a limited geographic area and relatively small number of individuals sampled, the true number of species within the *A. bifidus* species complex is undoubtably higher than the 5 SSHs from our analyses. Our results show consensus between molecular, morphological and phylogenetic data, allowing confident recognition of at least five species based on molecular data, and at least four species based on both molecular and morphological data. The congruence between molecular PSHs and particular morphotypes shows the importance of morphological vouchering as an integral part of species delimitation. Ideally, morphological vouchers are available for every specimen used for DNA

Fig. 4. Statistical parsimony TCS networks of *Astrotorhynchus* haplotypes in PopART. (A) TCS network of 28S rRNA haplotypes. (B) TCS network of COI haplotypes. Black dots represent missing connecting haplotypes, mutations between haplotypes are indicated by numbers. Colors within the circles indicate geographic origin. Colors outside the circles refer to the different species of *Astrotorhynchus* in Fig. 2. Circle sizes are proportional to the number of specimens with that haplotype. (For interpretation of the references to color in this figure legend, the reader is referred to the web version of this article.)

extraction, but this can be impractical for microscopic soft-bodied meiofauna. Photographs of diagnostic characters in live animals or dissection and recovery of the stylets prior to DNA extraction are therefore advisable. Distinct morphotypes, such as those of *A. bifidus* s. s., *A. regulatus* and *A. hakaiensis* n. sp. are relatively easy to recognize *a priori*, but subtle morphological variation such as in *A. intermedius* n. sp. was only discovered *a posteriori* when phylogenetic and molecular delimitation analyses suggested the existence of an additional species. Morphological vouchers from Friday Harbor, for which no molecular data are available, were initially lumped with *A. regulatus*, but can now be attributed to *A. intermedius* n. sp. Similarly, the collection of a larger number of specimens for molecular species delimitation in the Northeast Pacific was partly inspired by the recognition of conspicuously different morphotypes in the field, such as the finding of *A. hakaiensis* n. sp. on Calvert Island. As such, the interplay between molecular and morphological data facilitates the discovery of new species and pseudo-cryptic diversity.

4.3. Patterns of co-occurrence and life history

The different *Astrotorhynchus* species recognized here occur sympatrically on a regional (Northeastern Pacific) and local (sampling localities in British Columbia and Washington) scale (Fig. 1B). Different patterns of co-occurrence and co-existence have also been demonstrated in other meiofaunal species complexes (e.g., Derycke et al., 2016; Gabaldón et al., 2017). Several mechanisms have been proposed to explain these patterns, including (a) habitat partitioning defined by abiotic parameters such as depth, salinity, exposure, temperature, and substrate (e.g., Schizas et al., 2002), (b) trophic-niche partitioning coupled with the presence of distinct microbiomes (e.g., Derycke et al., 2016), (c) vulnerability to predation (e.g., Gabaldón et al., 2017), and (d) energy conservation strategies such as organ simplification, efficient reproduction structures and modes (hermaphroditism, internal fertilization, asexuality) and different generation times (e.g., Giere, 2009).

Little is known about feeding strategies and the life history of *A. bifidus* s. l. Many rhabdocoels prey on other meiofauna and personal observations on live specimens of *A. bifidus* s. l. have shown specimens feeding on copepods. First the animal circles around its prey, then it attaches its pharynx to the copepod somehow piercing or breaking the cuticle and sucking the content out. When finished, *Astrotorhynchus* detaches from the copepod leaving behind the empty cuticle (personal observation). It is possible that different species of *Astrotohrynchus* have different feeding strategies or prey preferences. Differential feeding strategies and species-specific microbiomes have been documented for sympatric bacterivorous nematode species within the *Litoditis marina* species complex (Derycke et al., 2016). High-throughput sequencing of gut contents and associated microbiomes could also test the idea of niche partitioning through selective feeding in the *A. bifidus* complex. Rhabdocoels are hermaphroditic and the complex male and female genital systems are the most important diagnostic characters for species identification. In many genera, species only differ from each other in the morphology of their stylet or other structures that are likely involved in sexual reproduction (e.g., bursal appendage). Sexual selection in hermaphroditic flatworms tends to involve traits enhancing fertilization success either during or after mating (Ramm, 2017). As such, the consistent differences in stylet morphology between the *Astrotorhynchus* species suggest that sexual reproduction and sexual selection might play an important role in speciation within the *A. bifidus* complex. Self-fertilization and asexual modes of reproduction (parthenogenesis, paratomy) are known to occur in other microturbellarians (Casu et al., 2012; Ramm et al., 2012; Rieger, 1986), but have not (yet) been evidenced in rhabdocoels.

Abiotic parameters could play a role in the occurrence and/or abundance of sympatric *Astrotorhynchus* species on a local and regional scale. Variation in these parameters can be spatial or temporal. For example, *A. hakaiensis* n. sp. and *A. regulatus* co-occur in the same kind of rocky intertidal in very sheltered bays or straits on Calvert Island and Quadra Island that receive freshwater input and organic influx from surrounding water catchment areas. *A. bifidus* s. s. was absent in these locations, but was instead found on Calvert Island's dynamic West Beach facing the open ocean; *A. hakaiensis* n. sp. was absent there. This demonstrates sympatric species are not necessarily syntopic. *A. bifidus* s. s. was the only species found on Calvert Island's West Beach and Bamfield, suggesting that this species is routinely subjected to stochastic perturbations, such as storms. This could increase the likelihood of passive dispersal through rafting and recruitment of new haplotypes within the same haplogroup, and partly explain the higher within-site haplotype diversity of *A. bifidus* s. s. in these exposed locations.

There are also some indications of seasonal specialization and succession. For instance, all *Astrotorhynchus* species, except for *A. hakaiensis* n. sp., co-occur in the sampling site in Victoria in February-March, with higher abundances of *A. regulatus* and *A. intermedius* n. sp. (Table 1; Fig. 2A). In November, only *A. bifidus* s. s. was found in Victoria. *A. bifidus* s. s. is either the only or most abundant species present during the summer and fall in Friday Harbor and Bamfield. Seasonal succession also occurs in other meiofaunal species complexes such as the rotifer *Brachionus plicatilis* s. l. (Gabaldón et al., 2017). Because our observations are preliminary, more elaborate sampling design, including seasonal monitoring in different locations, is necessary to test how seasonality, habitat and abiotic factors influences the occurrence and relative abundances of *Astrotorhynchus* species in the Northeast Pacific Ocean.

4.4. Biogeography

It is becoming increasingly clear that meiofaunal species complexes are often a mix of sympatric and allopatric species that can be widespread or have more restricted geographical ranges. Distributions of microturbellarians are poorly known and available data mostly reflect locations where taxonomic expertise, and thus routine sampling, exists (Curini-Galletti et al., 2012). Although only a small part of the known geographic range of *A. bifidus* s. l. was sampled for this study, our new data and distribution data from literature show that *A. intermedius* n. sp., *A. bifidus* s. s. and *A. regulatus* are present in both the Northern Atlantic and the Northern Pacific Oceans, often occurring sympatrically (e.g., West Greenland, Faroe Islands, Irish Sea, Swedish West Coast; Fig. 1A). *A. bifidus* s. s. is easily recognizable by the spines on its stylet, but the difference in stylet morphology between *A. intermedius* n. sp. and *A. regulatus* is more subtle. As such, it cannot be excluded that some historical records of *A. regulatus* are actually *A. intermedius* n. sp. *A. hakaiensis* n. sp. seems to be confined to the Northeast Pacific Ocean as no records are available for this species in the Northeast Atlantic Ocean, which is the most-studied area in the world for microturbellarians. The tri-oceanic distributions of the other *Astrotorhynchus* species could be the result of passive dispersal through rafting, as *A. bifidus* s. l. is very abundant in decaying algal matts in the swash zone (von Graff, 1882). Resting eggs attached to driftweed have also been recorded (pers. comm. David Fenwick). Although rafting on driftweed seems the most plausible mode of passive dispersal, ship ballast water and migrating birds could also play a role (Gerlach, 1977). Passive transoceanic transport maintaining gene flow among populations has also been suggested for epiphytic intertidal nematodes (Derycke et al., 2008). Molecular data from Atlantic and Arctic *A. bifidus* s. l. populations are needed to know whether gene flow is maintained between Pacific and Atlantic-Arctic populations or large genetic breakups occur suggesting long-term separation. In addition, some of these populations could constitute pseudo-cryptic or cryptic species themselves. At a regional scale, COI haplotypes of *A. bifidus* s. s. show no geographic structure and some haplotypes are shared between Bamfield and Friday Harbor, and between Friday Harbor and Calvert Island. This indicates regional dispersal is possible at scales of at least tens to hundreds of kilometers. COI haplotypes of *A. regulatus* show some preliminary geographic

structuring between specimens from Calvert Island and Victoria, but denser sampling is necessary to uncover population genetic structure on a regional scale.

4.5. Conclusions

By combining multiple DNA-based species delimitation approaches with phylogenetic analyses and comparative morphology, we were able to establish at least five species within the epiphytic rhabdocoel *Astrotorhynchus bifidus* s. l. in the Northeast Pacific Ocean. Molecular analyses included both nuclear (18S rRNA, 28S rRNA) and mitochondrial (COI) genes. Our newly developed rhabdocoel-specific COI barcode primers will allow future work to further explore the resolution of this gene in molecular phylogenetic inferences, species delimitation and DNA barcoding of other rhabdocoels. Multi-gene phylogenetic analyses, single-gene and multi-gene species delimitation methods, including ABGD, GMYC, PTP, STACEY and BBP, comparative stylet morphology and haplotype networks were used to formulate Primary Species Hypotheses (PSHs). After carefully considering the validity of each method and marker, the minimum consensus of all these approaches lead to Secondary Species Hypotheses (SSHs). At least four out of five SSHs could be diagnosed based on stylet morphology and are formally recognized as nominal species. All species occur sympatrically with at least one other species on a local and regional scale. On a larger spatial scale (North Atlantic, Northeast Pacific, and Arctic oceans), the *A. bifidus* complex seems to be a mix of allopatric (*A. hakaiensis* n. sp.) and sympatric (*A. bifidus* s. s., *A. regulatus*) species. However, the general lack of life history information such as modes of reproduction, development, dispersal potential, dormancy potential, habitat preferences and ecological tolerances hampers our understanding of speciation mechanisms and how they affect distribution patterns at different scales. We hypothesize that the tri-oceanic distribution of some species could be the result of high passive dispersal abilities through rafting on driftweed. As such, widespread species of seaweed-associated meiofauna do not conform to the meiofauna paradox.

Author contributions

NVS conceived the idea for this study, conducted the field sampling, generated and analyzed the data, and wrote the manuscript. ERH performed the molecular work and analyzed the morphological data. BSL wrote the manuscript and secured the funding.

Appendix A

Taxonomic account

PARAMESOSTOMINAE Luther, 1948
ASTROTORHYNCHUS von Graff, 1905
Mesostomum McIntosh, 1875
Gyrator Jensen, 1878
Pseudorhynchus von Graff, 1882

Provisional diagnosis (based on 'A. bifidus regulatus' by Luther, 1950*; see also* Karling et al., 1972*):* Paramesostominae with retractile proboscis and bifid posterior end provided with caudal glands. Pharynx situated in the middle of the body with a ciliated collar in the distal part of the lumen. Male genital system consists of paired testes, an unpaired extracapsular seminal vesicle, spermatic duct, copulatory bulb receiving prostate glands and provided with a tubiform, slightly funnel-shaped stylet surrounded by a spiral ridge. Paired ovaries and reticulate vitellaria connect to the common genital atrium by an afferent and efferent system. Common atrium with single gonopore and uterus. Afferent system with muscular bursa and spermatic duct connecting to the short common oviduct and vitelloduct. Efferent system with female duct and glands. Single gonopore. Uterus present.

Type species: Mesostomum bifidum McIntosh, 1875

Remarks: The diagnosis of the genus is derived from the morphological study of 'A. bifidus regulatus' by Luther (1950) and some remarks by Karling et al. (1972). Luther (1950) based his description on serial sections of 'A. bifidus regulatus' he received from Westblad and this is the most detailed morphological study of a species within the *A. bifidus* complex. Information on the internal organization of the atrial systems in the other species within the *A. bifidus* complex is currently lacking and the species diagnoses are mainly based on stylet morphology. As such, this provisional diagnosis of the genus *Astrotorhynchus* should be adapted if a detailed study on the the atrial organs of other species of *Astrotorhynchus* reveal consistent differences in internal morphology.

***Astrotorhynchus hakaiensis* n. sp.** (Fig. A1A)

Etymology: The species epithet refers to the Hakai Institute, which supports long-term scientific research on the coastal margin of British Columbia. In addition, the type locality Calvert Island lies within the Hakai Lúxvbálís Conservancy, the largest marine protected area on the BC coast.

Localities: Meay Inlet, Calvert Island, British Columbia, Canada (51°39′52″N, 128°05′47″W), algae in rocky lower intertidal (June 6, 2015; April 10, 2016; type locality). Hakai Institute Field Station, Quadra Island, British Columbia, Canada (50°06′53″N, 125°13′13″W), algae in rocky lower intertidal (April 26, 2017).

Type material: Nine whole mounts, one of which is designated as the holotype (BBM MI4059), the other ones are paratypes (BBM MI4060–MI4067). Genomic DNA of specimen CI38 also designated as paratype (BBM MI4058).

Other material: Observations on live animals. 18S rRNA (GenBank accession # MG256029–MG256030; MG256032–MG256033), 28S rRNA
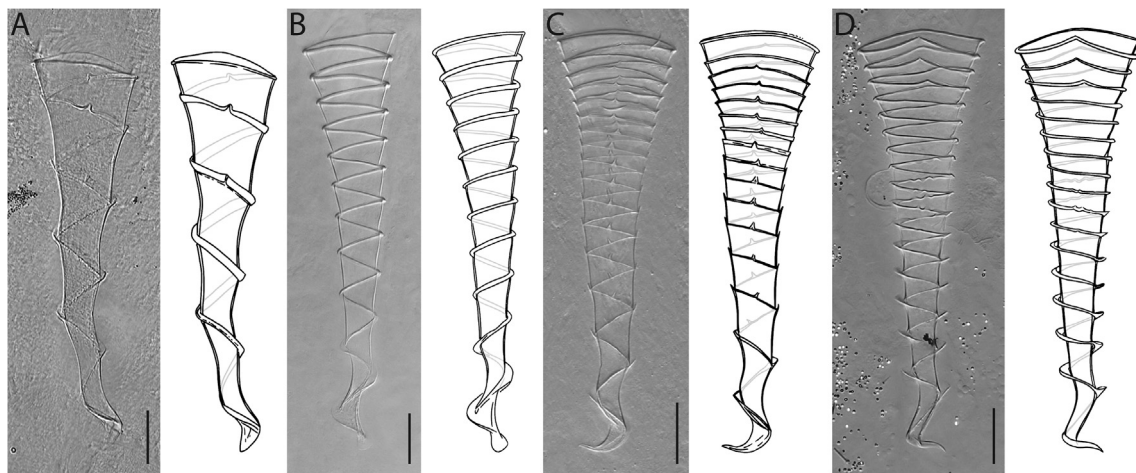
Fig. A1. Stylets from whole-mounted specimens of species within the *A. bifidus* s. l. complex. (A) *A. hakaiensis* n. sp. (B) *A. regulatus* (C) *A. bifidus* s. s. (D) *A. intermedius* n. sp. Scale bars are 20 μm.

(GenBank accession # MG256073–MG256074; MG256076–MG256077), COI (GenBank accession # MG256125–MG256126; MG256128–MG256129).

Diagnosis: Species of *Astrotorhynchus* with white-yellow coloration and (usually 2) bright-purple, subepidermal pigment bands, which run lengthwise or transversal along the dorsal side of the animal. Stylet 126–153 μm long, with short distal hook. Dexiotropic, spiral ridge with 5–5.5 windings, often with small spine-like features on 1 or 2 windings.

Remarks: Stylet measurements on 7 whole mounts ($\overline{x} = 143$ μm). In one specimen from Quadra Island the pigment was very pale and patchy. Similar color patterns (white-yellow with 2 purple bands) were observed in other epiphytic meiofauna, such as copepods and prolecithophorans, in the same samples. Subepidermal dorsal pigmentation is also common in other seaweed-associated rhabdocoels (e.g. several species of *Trigonostomum*), but to our knowledge the reason and nature of the pigmentation are unknown.

Astrotorhynchus regulatus (Fig. A1B)

Astrotorhynchus bifidus regulatus (McIntosh, 1875) von Graff, 1905

New localities: Clover Point, Victoria, British Columbia, Canada (48°24′12″N, 123°21′03″W), algae in rocky lower intertidal (March 20, 2015; September 2, 2015; March 3, 2016; February 5, 2017). Meay Inlet, Calvert Island, British Columbia, Canada (51°39′52″N, 128°05′47″W), algae in rocky lower intertidal (June 6, 2015). Hakai Institute Field Station, Quadra Island, British Columbia, Canada (50°06′53″N, 125°13′13″W), algae in rocky lower intertidal (April 26, 2017).

Other localities: See Fig. 1A.

Type material: Thirteen whole mounts, all designated as paratypes (BBM MI4069–MI4081). Genomic DNA of specimen Vic251 designated as paratype (BBM MI4068).

Other material: Observations on live animals. 18S rRNA (GenBank accession # MG256028; MG256031; MG256041–MG256043; MG256045–MG256051; MG256058; MG256060–MG256061; MG256064–MG256065), 28S rRNA (GenBank accession # MG256072; MG256075; MG256085–MG256087; MG256089–MG256095; MG256102; MG256104–MG256105; MG256108–MG256109), COI (GenBank accession # MG256124; MG256127; MG256144–MG256145; MG256147–MG256153; MG256160; MG256162–MG256163; MG256166).

Diagnosis: Species of *Astrotorhynchus* with orange-brown coloration. Stylet 161–200 μm long, with blunt distal end. Laeotropic, smooth spiral ridge with 10–13 windings.

Remarks: Stylet measurements on 13 whole mounts ($\overline{x} = 179$ μm). The two spines on the distal tip of the stylet in *A. bifidus regulatus* described by von Graff (1913) have not been observed in any of the whole mounts from British Columbia. Possibly this impression is caused by the often weak sclerotization of the blunt distal end leaving the edges of the widening spiral ridge more prominently visible.

Astrotorhynchus bifidus (McIntosh, 1875) von Graff, 1905 **s.s.** (Fig. A1C)

Astrotorhynchus bifidus bifidus (McIntosh, 1875) von Graff, 1905

New localities: Clover Point, Victoria, British Columbia, Canada (48°24′12″N, 123°21′03″W), algae in rocky lower intertidal (November 2, 2016; February 5, 2017). Friday Harbor, San Juan Island, Washington, USA (48°32′42″N, 123°00′44″W), algae on the dock of the marine station (October 8, 2016). West Beach boulders, Calvert Island, British Columbia, Canada (51°39′07″N, 128°08′33″W), algae in rocky lower intertidal (April 9, 2016). Dixon Island, Bamfield, British Columbia, Canada (48°51′05″N, 125°07′19″W), algae in rocky lower intertidal (July 2, 2015).

Other localities: See Fig. 1A.

Type material: Twelve whole mounts, all designated as paratypes (BBM MI4083– MI4094). Genomic DNA of specimen Vic242 designated as paratype (BBM MI4082).

Other material: Observations on live animals. 18S rRNA (GenBank accession # MG256034; MG256052–MG256056; MG256066; MG256024–MG256027; MG256035–MG256038), 28S rRNA (GenBank accession # MG256078; MG256096–MG256100; MG256110; MG256067–MG256071; MG256079–MG256082), COI (GenBank accession # MG256130; MG256154–MG256158; MG256167; MG256115–MG256119; MG256132–MG256135).

Diagnosis: Species of *Astrotorhynchus* with orange-brown coloration. Stylet 137–185 μm long, with sharp distal hook. Dexiotropic, spiral ridge with 13–18 windings, most of which have prominent spines.

Remarks: Stylet measurements on 12 whole mounts ($\overline{x} = 154$ μm).

Astrotorhynchus intermedius **n. sp.** (Fig. A1D)

Etymology: The species epithet refers to the morphology of the stylet, which shows mixed characters from both *A. bifidus* s. s. and *A. regulatus*.

Localities: Clover Point, Victoria, British Columbia, Canada (48°24′12″N, 123°21′03″W), algae in rocky lower intertidal (February 5, 2017; type locality). Friday Harbor, San Juan Island, Washington, USA (48°32′42″N, 123°00′44″W), algae on the dock of the marine station (October 8, 2016).

Other localities: Swedish West Coast, Sweden (Van Steenkiste et al., 2013).

Type material: Three whole mounts, one of which is designated as the holotype (BBM MI4097), the other two are paratypes (BBM MI4096; BBM MI4098). Genomic DNA of specimen Vic249 designated as paratype (BBM MI4095).

Other material: Observations on live animals. 18S rRNA (GenBank accession # MG256057; MG256059; MG256062–MG256063), 28S rRNA (GenBank accession # MG256101; MG256103; MG256106–MG256107), COI (GenBank accession # MG256159; MG256161; MG256164–MG256165).

Diagnosis: Species of *Astrotorhynchus* with orange-brown coloration. Stylet 150–153 μm long, with sharp distal hook. Dexiotropic, spiral ridge with 16–17 windings, of which the proximal four are pointed. Windings 8–11 have a wavy edge.

Remarks: Stylet measurements on 3 whole mounts ($\overline{x} = 152$ μm). The whole mount from Friday Harbour has the typical wavy edge on windings 8–11 of the spiral ridge, but lacks the pointy edge on the first four windings.

Key to the species within the A. bifidus s. l. complex

1. Stylet with 5–5.5 windings, often with small spine-like features on 1 or 2 windings. Adult animals with white-yellow coloration and (usually 2) bright-purple, subepidermal pigment bands .... ***A. hakaiensis*** **n. sp.**

Stylet with more than 10 windings. Adult animals transparent to orange-brown 2

2. Stylet with blunt distal end and 10–13 laeotropic windings .... ***A. regulatus***

Stylet with distal hook and 13–18 dexiotropic windings 3

3. Most stylet windings have prominent spines .... ***A. bifidus*** **s. s.**

Proximal 4 stylet windings pointed. Windings 8–11 with wavy edge ..... ***A. intermedius*** **n. sp.**

Appendix B. Supplementary material

DNA sequence data: Genbank accession numbers and data on each individual (identifier, sampling locality, coordinates, collection date) in Table 1, Tables S1 and S4.

Museum vouchers: BBM accession numbers for the morphological vouchers and additional information on sampling locations, collection dates and type material in the Appendix A and supporting information.

Supplementary data associated with this article can be found, in the online version, at https://doi.org/10.1016/j.ympev.2017.12.012.

References

Adams, M., Raadik, T.A., Burridge, C.P., Georges, A., 2014. Global biodiversity assessment and hyper-cryptic species complexes: More than one species of elephant in the room? Syst. Biol. 63, 518–533. http://dx.doi.org/10.1093/sysbio/syu017.

Appeltans, W., Ahyong, S.T., Anderson, G., Angel, M.V., Artois, T., Bailly, N., Bamber, R., Barber, A., Bartsch, I., Berta, A., Błażewicz-Paszkowycz, M., Bock, P., Boxshall, G., Boyko, C.B., Brandão, S.N., Bray, R.a., Bruce, N.L., Cairns, S.D., Chan, T.-Y., Cheng, L., Collins, A.G., Cribb, T., Curini-Galletti, M., Dahdouh-Guebas, F., Davie, P.J.F., Dawson, M.N., De Clerck, O., Decock, W., De Grave, S., de Voogd, N.J., Domning, D.P., Emig, C.C., Erséus, C., Eschmeyer, W., Fauchald, K., Fautin, D.G., Feist, S.W., Fransen, C.H.J.M., Furuya, H., Garcia-Alvarez, O., Gerken, S., Gibson, D., Gittenberger, A., Gofas, S., Gómez-Daglio, L., Gordon, D.P., Guiry, M.D., Hernandez, F., Hoeksema, B.W., Hopcroft, R.R., Jaume, D., Kirk, P., Koedam, N., Koenemann, S., Kolb, J.B., Kristensen, R.M., Kroh, A., Lambert, G., Lazarus, D.B., Lemaitre, R., Longshaw, M., Lowry, J., Macpherson, E., Madin, L.P., Mah, C., Mapstone, G., McLaughlin, P.a., Mees, J., Meland, K., Messing, C.G., Mills, C.E., Molodtsova, T.N., Mooi, R., Neuhaus, B., Ng, P.K.L., Nielsen, C., Norenburg, J., Opresko, D.M., Osawa, M., Paulay, G., Perrin, W., Pilger, J.F., Poore, G.C.B., Pugh, P., Read, G.B., Reimer, J.D., Rius, M., Rocha, R.M., Saiz-Salinas, J.I., Scarabino, V., Schierwater, B., Schmidt-Rhaesa, A., Schnabel, K.E., Schotte, M., Schuchert, P., Schwabe, E., Segers, H., Self-Sullivan, C., Shenkar, N., Siegel, V., Sterrer, W., Stöhr, S., Swalla, B., Tasker, M.L., Thuesen, E.V., Timm, T., Todaro, M.A., Turon, X., Tyler, S., Uetz, P., van der Land, J., Vanhoorne, B., van Ofwegen, L.P., van Soest, R.W.M., Vanaverbeke, J., Walker-Smith, G., Walter, T.C., Warren, A., Williams, G.C., Wilson, S.P., Costello, M.J., 2012. The magnitude of global marine species diversity. Curr. Biol. 22, 2189–2202. http://dx.doi.org/10.1016/j.cub.2012.09.036.

Artois, T., Fontaneto, D., Hummon, W.D., McInnes, S.J., Todaro, M.A., Sørensen, M.V., Zullini, A., 2011. Ubiquity of microscopic animals? Evidence from the morphological approach in species identification. In: Fontaneto, D. (Ed.), Biogeography of Microscopic Organisms, Is Everything Small Everywhere? Systematics Association & Cambridge University Press, Cambridge, pp. 244–283.

Ax, P., 2008. Plathelminthes aus Brackgewässern der Nordhalbkugel. Franz Steiner Verlag, Stuttgart.

Baker, J.M., Funch, P., Giribet, G., 2007. Cryptic speciation in the recently discovered American cycliophoran *Symbion americanus*; genetic structure and population expansion. Mar. Biol. 151, 2183–2193. http://dx.doi.org/10.1007/s00227-007-0654-8.

Bouckaert, R., Heled, J., Kühnert, D., Vaughan, T., Wu, C.H., Xie, D., Suchard, M.A., Rambaut, A., Drummond, A.J., 2014. BEAST 2: A software platform for Bayesian evolutionary analysis. PLoS Comput. Biol. 10, e1003537. http://dx.doi.org/10.1371/journal.pcbi.1003537.

Carugati, L., Corinaldesi, C., Dell'Anno, A., Danovaro, R., 2015. Metagenetic tools for the census of marine meiofaunal biodiversity: an overview. Mar. Genomics 24, 11–20. http://dx.doi.org/10.1016/j.margen.2015.04.010.

Casu, M., Cossu, P., Lai, T., Scarpa, F., Sanna, D., Dedola, G.L., Curini-Galletti, M., 2012. First evidence of self-fertilization in a marine microturbellarian (Platyhelminthes). J. Exp. Mar. Bio. Ecol. 428, 32–38. http://dx.doi.org/10.1016/j.jembe.2012.05.026.

Casu, M., Curini-Galletti, M., 2004. Sibling species in interstitial flatworms: a case study using *Monocelis lineata* (Proseriata: Monocelididae). Mar. Biol. 145, 669–679. http://dx.doi.org/10.1007/s00227-004-1367-x.

Clement, M., Posada, D., Crandall, K.A., 2000. TCS: a computer program to estimate gene genealogies. Mol. Ecol. 9, 1657–1659. http://dx.doi.org/10.1046/j.1365-294X.2000.01020.x.

Curini-Galletti, M., Artois, T., Delogu, V., de Smet, W.H., Fontaneto, D., Jondelius, U., Leasi, F., Martínez, A., Meyer-Wachsmuth, I., Nilsson, K.S., Tongiorgi, P., Worsaae, K., Todaro, M.A., 2012. Patterns of diversity in soft-bodied meiofauna: dispersal ability and body size matter. PLoS One 7, e33801. http://dx.doi.org/10.1371/journal.pone.0033801.

Curini-Galletti, M., Puccinelli, I., 1998. The *Gyratrix hermaphroditus* species complex (Kalyptorhynchia: Polycystididae) in marine habitats of eastern Australia. Hydrobiologia 383, 287–298. http://dx.doi.org/10.1023/A:1003456102035.

De Queiroz, K., 2007. Species concepts and species delimitation. Syst. Biol. 56, 879–886. http://dx.doi.org/10.1080/10635150701701083.

Delogu, V., Curini-Galletti, M., 2009. The *Parotoplana jondelii* species-group (Platyhelminthes: Proseriata): a microturbellarian radiation in the Mediterranean. Contrib. Zool. 78, 99–112.

Derycke, S., De Meester, N., Rigaux, A., Creer, S., Bik, H., Thomas, W.K., Moens, T., 2016. Coexisting cryptic species of the *Litoditis marina* complex (Nematoda) show differential resource use and have distinct microbiomes with high intraspecific variability. Mol. Ecol. 25, 2093–2110. http://dx.doi.org/10.1111/mec.13597.

Derycke, S., Remerie, T., Backeljau, T., Vierstraete, A., Vanfleteren, J., Vincx, M., Moens, T., 2008. Phylogeography of the *Rhabditis (Pellioditis) marina* species complex: evidence for long-distance dispersal, and for range expansions and restricted gene flow in the northeast Atlantic. Mol. Ecol. 17, 3306–3322. http://dx.doi.org/10.1111/j.1365-294X.2008.03846.x.

Fenchel, T., Finlay, B.J., 2004. The ubiquity of small species: patterns of local and global diversity. Bioscience 54, 777. http://dx.doi.org/10.1641/0006-3568(2004)054[0777:TUOSSP]2.0.CO;2.

Finlay, B.J., 2002. Global dispersal of free-living microbial eukaryote species. Science 296, 1061–1063. http://dx.doi.org/10.1126/science.1070710.

Fonseca, V.G., Carvalho, G.R., Sung, W., Johnson, H.F., Power, D.M., Neill, S.P., Packer, M., Blaxter, M.L., Lambshead, P.J.D., Thomas, W.K., Creer, S., 2010. Second-generation environmental sequencing unmasks marine metazoan biodiversity. Nat. Commun. 1, 98. http://dx.doi.org/10.1038/ncomms1095.

Fontaneto, D., 2011. Biogeography of Microscopic Organisms: is Everything Small Everywhere?, Biogeography of Microscopic Organisms. Systematics Association & Cambridge University Press, Cambridge doi:10.1017/CBO9780511974878.

Fontaneto, D., Flot, J.-F., Tang, C.Q., 2015. Guidelines for DNA taxonomy, with a focus on the meiofauna. Mar. Biodivers 45, 433–451.

Gabaldón, C., Fontaneto, D., Carmona, M.J., Montero-Pau, J., Serra, M., 2017. Ecological differentiation in cryptic rotifer species: what we can learn from the *Brachionus plicatilis* complex. Hydrobiologia. http://dx.doi.org/10.1007/s10750-016-2723-9.

Garlitska, L., Neretina, T., Schepetov, D., Mugue, N., De Troch, M., Baguley, J.G., Azovsky, A., 2012. Cryptic diversity of the "cosmopolitan" harpacticoid copepod *Nannopus palustris*: Genetic and morphological evidence. Mol. Ecol. 21, 5336–5347. http://dx.doi.org/10.1111/mec.12016.

Gerlach, S., 1977. Means of meiofaunal dispersal. Microfauna Meeresboden 61, 89–103.

Giere, O., 2009. Introduction to meiobenthology. Meiobenthology: the microscopic motile fauna of aquatic sediments, Second. ed. Springer-Verlag, Berlin, Heidelberg.

Gómez, A., Serra, M., Carvalho, G.R., Lunt, D.H., 2002. Speciation in ancient cryptic species complexes: evidence from the molecular phylogeny of *Brachionus plicatilis* (Rotifera). Evolution (N.Y) 56, 1431–1444.

Heled, J., Drummond, A.J., 2010. Bayesian inference of species trees from multilocus data. Mol. Biol. Evol. 27, 570–580. http://dx.doi.org/10.1093/molbev/msp274.

Hillis, D.M., Bull, J.J., 1993. An empirical test of bootstrapping as a method for assessing confidence in phylogenetic analysis. Syst. Biol. 42, 182–192. http://dx.doi.org/10.1093/sysbio/42.2.182.

Huelsenbeck, J.P., Rannala, B., 2004. Frequentist properties of bayesian posterior probabilities of phylogenetic trees under simple and complex substitution models. Syst. Biol. 53, 904–913. http://dx.doi.org/10.1080/10635150490522629.

Jensen, O., 1878. Turbellaria ad litora Norvegiae Occidentalia. Turbellarier ved Norges Vestkyst. J W Eided Bogtrykkeri, Bergen.

Jones, G., 2017. Algorithmic improvements to species delimitation and phylogeny estimation under the multispecies coalescent. J. Math. Biol. 74, 447. http://dx.doi.org/10.1007/s00285-016-1034-0.

Jones, G., Aydin, Z., Oxelman, B., 2015. DISSECT: An assignment-free Bayesian discovery method for species delimitation under the multispecies coalescent. Bioinformatics 31, 991–998. http://dx.doi.org/10.1093/bioinformatics/btu770.

Jörger, K.M., Norenburg, J.L., Wilson, N.G., Schrödl, M., 2012. Barcoding against a paradox? Combined molecular species delineations reveal multiple cryptic lineages in elusive meiofaunal sea slugs. BMC Evol. Biol. 12, 245. http://dx.doi.org/10.1186/1471-2148-12-245.

Karling, T.G., 1986. Free-living marine Rhabdocoela (Platyhelminthes) from the N. American Pacific coast. With remarks on species from other areas. Zool. Scr. 15, 201–219.

Karling, T.G., 1967. On the genus *Promesostoma* (Turbellaria), with descriptions of four new species from Scandinavia and California. Sarsia 29, 257–268.

Karling, T.G., Mack-Fira, V., Dörjes, J., 1972. First report on marine microturbellarians from Hawaii. Zool. Scr. 1, 251–269. http://dx.doi.org/10.1111/j.1463-6409.1972.tb00575.x.

Katoh, K., Toh, H., 2008. Improved accuracy of multiple ncRNA alignment by incorporating structural information into a MAFFT-based framework. BMC Bioinf. 9, 212. http://dx.doi.org/10.1186/1471-2105-9-212.

Kearse, M., Moir, R., Wilson, A., Stones-Havas, S., Cheung, M., Sturrock, S., Buxton, S., Cooper, A., Markowitz, S., Duran, C., Thierer, T., Ashton, B., Meintjes, P., Drummond, A.A., 2012. Geneious Basic: An integrated and extendable desktop software platform for the organization and analysis of sequence data. Bioinformatics. http://dx.doi.org/10.1093/bioinformatics/bts199.

Kieneke, A., Martínez Arbizu, P.M., Fontaneto, D., 2012. Spatially structured populations with a low level of cryptic diversity in European marine gastrotricha. Mol. Ecol. 21, 1239–1254. http://dx.doi.org/10.1111/j.1365-294X.2011.05421.x.

Kueck, P., 2009. ALICUT: a Perlscript which cuts ALISCORE identified RSS, version 2.0 edn. [WWW Document]. URL < http://www.zfmk.utilities.de > .

Kumar, S., Stecher, G., Tamura, K., 2016. MEGA7: Molecular Evolutionary Genetics Analysis version 7.0 for bigger datasets. Mol. Biol. Evol. 33, 1870–1874. http://dx.doi.org/10.1093/molbev/msw054.

Lanfear, R., Calcott, B., Ho, S.Y.W., Guindon, S., 2012. PartitionFinder: Combined selection of partitioning schemes and substitution models for phylogenetic analyses. Mol. Biol. Evol. 29, 1695–1701. http://dx.doi.org/10.1093/molbev/mss020.

Leasi, F., Andrade, S.C.D.S., Norenburg, J., 2016. At least some meiofaunal species are not everywhere. Indication of geographic, ecological and geological barriers affecting the dispersion of species of *Ototyphlonemertes* (Nemertea, Hoplonemertea). Mol. Ecol. 25, 1381–1397. http://dx.doi.org/10.1111/mec.13568.

Leasi, F., Norenburg, J.L., 2014. The necessity of DNA taxonomy to reveal cryptic diversity and spatial distribution of meiofauna, with a focus on nemertea. PLoS One 9, e104385. http://dx.doi.org/10.1371/journal.pone.0104385.

Luther, A., 1950. Untersuchungen an Rhabdocoelen Turbellarien. IX. Zur Kenntnis einiger Typhloplaniden. X. Über *Astrotorhynchus bifidus* (M'Int.). Acta Zool. Fenn. 60, 3–42.

Luther, A., 1948. Untersuchungen an Rhabdocoelen Turbellarien. VII. Über einige marine Dalyellioida. VIII. Beiträge zur Kenntnis der Typhloplanoida. Acta Zool. Fenn. 55, 3–122.

Luther, A., 1943. Untersuchungen an Rhabdocoelen Turbellarien. IV. Über einige Repräsentanten der Familie Proxenetidae. Acta Zool. Fenn. 43, 3–100.

McIntosh, W.C., 1875. The marine invertebrates and fishes of St. Andrews. Taylor & Francis, London.

Meyer-Wachsmuth, I., Curini Galletti, M., Jondelius, U., 2014. Hyper-cryptic marine meiofauna: species complexes in Nemertodermatida. PLoS One 9, e107688. http://dx.doi.org/10.1371/journal.pone.0107688.

Misof, B., Misof, K., 2009. A Monte Carlo approach successfully identifies randomness in multiple sequence alignments: a more objective means of data exclusion. Syst. Biol. 58, 21–34. http://dx.doi.org/10.1093/sysbio/syp006.

Noren, M., Jondelius, U., 2002. The phylogenetic position of the Prolecithophora (Rhabditophora, "Platyhelminthes"). Zool. Scr. 31, 403–414. http://dx.doi.org/10.1046/j.1463-6409.2002.00082.x.

Pons, J., Barraclough, T.G., Gomez-Zurita, J., Cardoso, A., Duran, D.P., Hazell, S., Kamoun, S., Sumlin, W.D., Vogler, A.P., 2006. Sequence-based species delimitation for the DNA taxonomy of undescribed insects. Syst. Biol. 55, 595–609. http://dx.doi.org/10.1080/10635150600852011.

Puillandre, N., Lambert, A., Brouillet, S., Achaz, G., 2012a. ABGD, Automatic Barcode Gap Discovery for primary species delimitation. Mol. Ecol. 21, 1864–1877. http://dx.doi.org/10.1111/j.1365-294X.2011.05239.x.

Puillandre, N., Modica, M.V., Zhang, Y., Sirovich, L., Boisselier, M.C., Cruaud, C., Holford, M., Samadi, S., 2012b. Large-scale species delimitation method for hyperdiverse groups. Mol. Ecol. 21, 2671–2691. http://dx.doi.org/10.1111/j.1365-294X.2012.05559.x.

Rambaut, A., Suchard, M.A., Xie, D., Drummond, A.J., n.d. Tracer v1.6 [WWW Document]. URL http://beast.bio.ed.ac.uk/Tracer.

Ramm, S.A., 2017. Exploring the sexual diversity of flatworms: ecology, evolution, and the molecular biology of reproduction. Mol. Reprod. Dev. http://dx.doi.org/10.1002/mrd.22669.

Ramm, S.A., Vizoso, D.B., Schärer, L., 2012. Occurrence, costs and heritability of delayed selfing in a free-living flatworm. J. Evol. Biol. 25, 2559–2568. http://dx.doi.org/10.1111/jeb.12012.

Reid, N.M., Carstens, B.C., 2012. Phylogenetic estimation error can decrease the accuracy of species delimitation: a Bayesian implementation of the general mixed Yule-coalescent model. BMC Evol. Biol. 12, 196. http://dx.doi.org/10.1186/1471-2148-12-196.

Rieger, R.M., 1986. Asexual reproduction and the turbellarian archetype. Hydrobiologia 132, 35–45.

Ronquist, F., Huelsenbeck, J.P., 2003. MrBayes 3: Bayesian phylogenetic inference under mixed models. Bioinformatics 19, 1572–1574. http://dx.doi.org/10.1093/bioinformatics/btg180.

Scarpa, F., Cossu, P., Lai, T., Sanna, D., Curini-Galletti, M., Casu, M., 2016. Meiofaunal cryptic species challenge species delimitation: the case of the *Monocelis lineata* (Platyhelminthes: Proseriata) species complex. Contrib. Zool. 85, 123–145.

Schizas, N.V., Coull, B.C., Chandler, G.T., Quattro, J.M., 2002. Sympatry of distinct mitochondrial DNA lineages in a copepod inhabiting estuarine creeks in the southeastern USA. Mar. Biol. 140, 585–594. http://dx.doi.org/10.1007/s00227-001-0728-y.

Schockaert, E.R., 1996. Turbellarians. In: Hall, G. (Ed.), Methods for the Examination of Organismal Diversity in Soils and Sediments. CAB International, Wallingford, pp. 211–225.

Snelgrove, P.V.R., 1999. Getting to the bottom of marine biodiversity: Sedimentary habitats: Ocean bottoms are the most widespread habitat on Earth and support high biodiversity and key ecosystem services. Bioscience 49, 129–138. http://dx.doi.org/10.2307/1313538.

Stamatakis, A., 2014. RAxML version 8: A tool for phylogenetic analysis and post-analysis of large phylogenies. Bioinformatics 30, 1312–1313. http://dx.doi.org/10.1093/bioinformatics/btu033.

Tang, C.Q., Leasi, F., Obertegger, U., Kieneke, A., Barraclough, T.G., Fontaneto, D., 2012. The widely used small subunit 18S rDNA molecule greatly underestimates true diversity in biodiversity surveys of the meiofauna. Proc. Natl. Acad. Sci. 109, 16208–16212. http://dx.doi.org/10.1073/pnas.1209160109.

Tessens, B., 2012. Dealing with a taxonomic Gordian knot: phylogeny of and cryptic diversity in *Gyratrix hermaphroditus* Ehrenberg, 1831 (Platyhelminthes: Rhabdocoela, Kalyptorhynchia). Hasselt University, Hasselt, Belgium.

Tessens, B., Janssen, T., Artois, T., 2014. Molecular phylogeny of Kalyptorhynchia (Rhabdocoela, Platyhelminthes) inferred from ribosomal sequence data. Zool. Scr. 43, 519–530. http://dx.doi.org/10.1111/zsc.12066.

Van Steenkiste, N., Locke, S.A., Castelin, M., Marcogliese, D.J., Abbott, C.L., 2015. New primers for DNA barcoding of digeneans and cestodes (Platyhelminthes). Mol. Ecol. Resour. 15, 945–952. http://dx.doi.org/10.1111/1755-0998.12358.

Van Steenkiste, N., Tessens, B., Willems, W., Backeljau, T., Jondelius, U., Artois, T., 2013. A comprehensive molecular phylogeny of Dalytyphloplanida (Platyhelminthes: Rhabdocoela) reveals multiple escapes from the marine environment and origins of symbiotic relationships. PLoS One 8, e59917. http://dx.doi.org/10.1371/journal.pone.0059917.

Van Steenkiste, N.W.L., Leander, B.S., 2017. Molecular phylogeny of trigonostomine turbellarians (Platyhelminthes: Rhabdocoela: Trigonostomidae), including four new species from the Northeast Pacific Ocean. Zool. J. Linn. Soc. http://dx.doi.org/10.1093/zoolinnean/zlx046. zlx046 (in press).

Vanhove, M.P.M., Tessens, B., Schoelinck, C., Jondelius, U., Littlewood, D.T.J., Artois, T., Huyse, T., 2013. Problematic barcoding in flatworms: A case-study on monogeneans and rhabdocoels (Platyhelminthes). Zookeys 365, 355–379. http://dx.doi.org/10.3897/zookeys.365.5776.

von Graff, L., 1913. Das Tierreich 35. Turbellaria II. Rhabdocoelida. Verlag von R. Friedländer und Sohn, Berlin.

von Graff, L., 1905. Marine Turbellarien Orotavas und der Küsten Europas. Ergebnisse einiger, mit Unterstützung der kais. Akademie der Wissenschaften in Wien (aus dem Legate Wedl) in den Jahren 1902 und 1903 unternommen Studienreise. II. Rhabdocoela. Zeitschrift für Wissenschaftlichen Zool. 83, 68–148.

von Graff, L., 1882. Monographie der Turbellarien. I. Rhabdocoelida. Verlag von Wilhelm Engelmann, Leipzig.

Westheide, W., Schmidt, H., 2003. Cosmopolitan versus cryptic meiofaunal polychaete species: an approach to a molecular taxonomy. Helgol. Mar. Res. 57, 1–6. http://dx.doi.org/10.1007/s10152-002-0114-2.

Willems, W.R., Artois, T.J., Vermin, W.A., Schockaert, E.R., 2004. Revision of *Trigonostomum* Schmidt, 1852 (Platyhelminthes, Typhloplanoida, Trigonostomidae) with the description of seven new species. Zool. J. Linn. Soc. 141, 271–296. http://dx.doi.org/10.1111/j.1096-3642.2004.00124.x.

Yang, Z., 2015. The BPP program for species tree estimation and species delimitation.

Curr. Zool. 61, 854–865. http://dx.doi.org/10.1093/czoolo/61.5.854.

Zeppilli, D., Sarrazin, J., Leduc, D., Arbizu, P.M., Fontaneto, D., Fontanier, C., Gooday, A.J., Kristensen, R.M., Ivanenko, V.N., Sørensen, M.V., Vanreusel, A., Thébault, J., Mea, M., Allio, N., Andro, T., Arvigo, A., Castrec, J., Danielo, M., Foulon, V., Fumeron, R., Hermabessiere, L., Hulot, V., James, T., Langonne-Augen, R., Le Bot, T., Long, M., Mahabror, D., Morel, Q., Pantalos, M., Pouplard, E., Raimondeau, L., Rio-Cabello, A., Seite, S., Traisnel, G., Urvoy, K., Van Der Stegen, T., Weyand, M., Fernandes, D., 2015. Is the meiofauna a good indicator for climate change and anthropogenic impacts? Mar. Biodivers. 45, 505–535. http://dx.doi.org/10.1007/s12526-015-0359-z.

Zhang, J., Kapli, P., Pavlidis, P., Stamatakis, A., 2013. A general species delimitation method with applications to phylogenetic placements. Bioinformatics 29, 2869–2876. http://dx.doi.org/10.1093/bioinformatics/btt499.